JGR Oceans

RESEARCH ARTICLE
10.1029/2023JC020513

The Northeast Water Polynya, Greenland: Climatology, Atmospheric Forcing and Ocean Response

Miriam G. Bennett[1], **Ian A. Renfrew**[1], **David P. Stevens**[2], **and G. W. K. Moore**[3]

[1]School of Environmental Sciences, University of East Anglia, Norwich, UK, [2]School of Mathematics, University of East Anglia, Norwich, UK, [3]School of the Environment, University of Toronto, Toronto, ON, Canada

Key Points:

- A climatological study of the Northeast Water Polynya reveals spatial, interannual and decadal variability
- The summertime polynya extent closely correlates to near-surface winds, largely dictated by the orientation of the pressure gradient across Fram Strait
- Between 1980 and 2022, the duration of the Northeast Water Polynya, and associated oceanic warming, increased

Correspondence to:

M. G. Bennett,
miriam.bennett@uea.ac.uk

Citation:

Bennett, M. G., Renfrew, I. A., Stevens, D. P., & Moore, G. W. K. (2024). The Northeast Water Polynya, Greenland: Climatology, atmospheric forcing and ocean response. *Journal of Geophysical Research: Oceans*, *129*, e2023JC020513. https://doi.org/10.1029/2023JC020513

Received 22 SEP 2023
Accepted 8 APR 2024

Author Contributions:

Conceptualization: Ian A. Renfrew, David P. Stevens, G. W. K. Moore
Formal analysis: Miriam G. Bennett
Funding acquisition: Ian A. Renfrew
Investigation: Miriam G. Bennett
Methodology: Miriam G. Bennett, Ian A. Renfrew, David P. Stevens, G. W. K. Moore
Supervision: Ian A. Renfrew, David P. Stevens, G. W. K. Moore
Visualization: Miriam G. Bennett
Writing – original draft: Miriam G. Bennett
Writing – review & editing: Miriam G. Bennett, Ian A. Renfrew, David P. Stevens, G. W. K. Moore

Abstract The Northeast Water Polynya is a significant annually recurring summertime Arctic polynya, located off the coast of Northeast Greenland. It is important for marine wildlife and affects local atmospheric and oceanic processes. In this study, over 40 years of observational and reanalysis products (ERA5 and ORAS5) are analyzed to characterize the polynya's climatology and ascertain forcing mechanisms. The Northeast Water Polynya has high spatiotemporal variability; its location, size and structure vary interannually, and the period for which it is open is changing. We show this variability is largely driven by atmospheric forcing. The polynya extent is determined by the direction of the near-surface flow regime, and the relative locations of high and low sea-level pressure centers over the region. The surface conditions also impact the oceanic water column, which has a strong seasonal cycle in potential temperature and salinity, the amplitude of which decreases with depth. The ocean reanalyses also show a significant warming trend at all depths and a freshening near the surface consistent with greater ice melt, but salinification at lower depths (~200 m). As the Arctic region changes due to anthropogenic forcing, the sea-ice edge is migrating northwards and the Northeast Water Polynya is generally opening earlier and closing later in the year. This could have significant implications for both the atmosphere and ocean in this complex and rapidly changing environment.

Plain Language Summary Polynya's are areas of open water surrounded by sea ice. These features are important for marine wildlife and can impact how the atmosphere and ocean interact. The Northeast Water Polynya is one example from the Arctic. Each summer, it appears off the coast of Northeast Greenland. In this research we use data from the last 40 years to study this polynya. We find that its location, size and structure varies from year to year. The period for which it is open each year also changes. We conclude that these differences are due to changes in the wind direction near the surface. Winds that flow from south to north over the region are linked to a larger polynya. Winds that flow from north to south are linked to a smaller polynya. With climate change, the Northeast Water Polynya is opening earlier and closing later in the year. In the future, this polynya may no longer form as it does now, which will impact the local environment and wildlife.

1. Introduction

The Northeast Water (NEW) Polynya is an important sea ice feature of the Arctic. A region of open water, surrounded by sea ice, it is situated to the Northwest of Fram Strait, over the Ob Bank continental shelf, off the coast of the Nørdoststrundingen headland of Northeast Greenland (Figure 1). Its center is often located between longitudes of 5°W and 15°W and latitudes of 77°N and 81°N (Barber & Massom, 2007), but the shape and position of the polynya varies on seasonal, interannual and decadal time scales. It has a maximum areal extent of approximately 44,000 km^2 (Barber & Massom, 2007) and plays an important role in summertime atmosphere-ocean interaction for the northern European Arctic (Deming, 1993). In previous literature it has been described as a stable, annually recurring polynya that forms as a result of ice barriers both to the north and south that limit heavy ice intrusion, coupled with strong and persistent northerly winds advecting sea-ice away from the coast (e.g., Barber & Massom, 2007; Speer et al., 2017; Tamura & Ohshima, 2011). However, there has been little observational evidence to confirm these descriptions, particularly in more recent years, and with the climate of the Arctic quickly changing due to anthropogenic forcing, this study aims to provide a first comprehensive climatology of the NEW Polynya, and examine its drivers and its evolution over the last few decades.

The NEW Polynya develops during most summer seasons, to various extents, and is considered one of the largest and most consistently recurring polynyas of the Arctic summer, thus having a significant impact on local atmospheric, oceanographic and biological processes (Deming, 1993). It is known to be a site of elevated biological

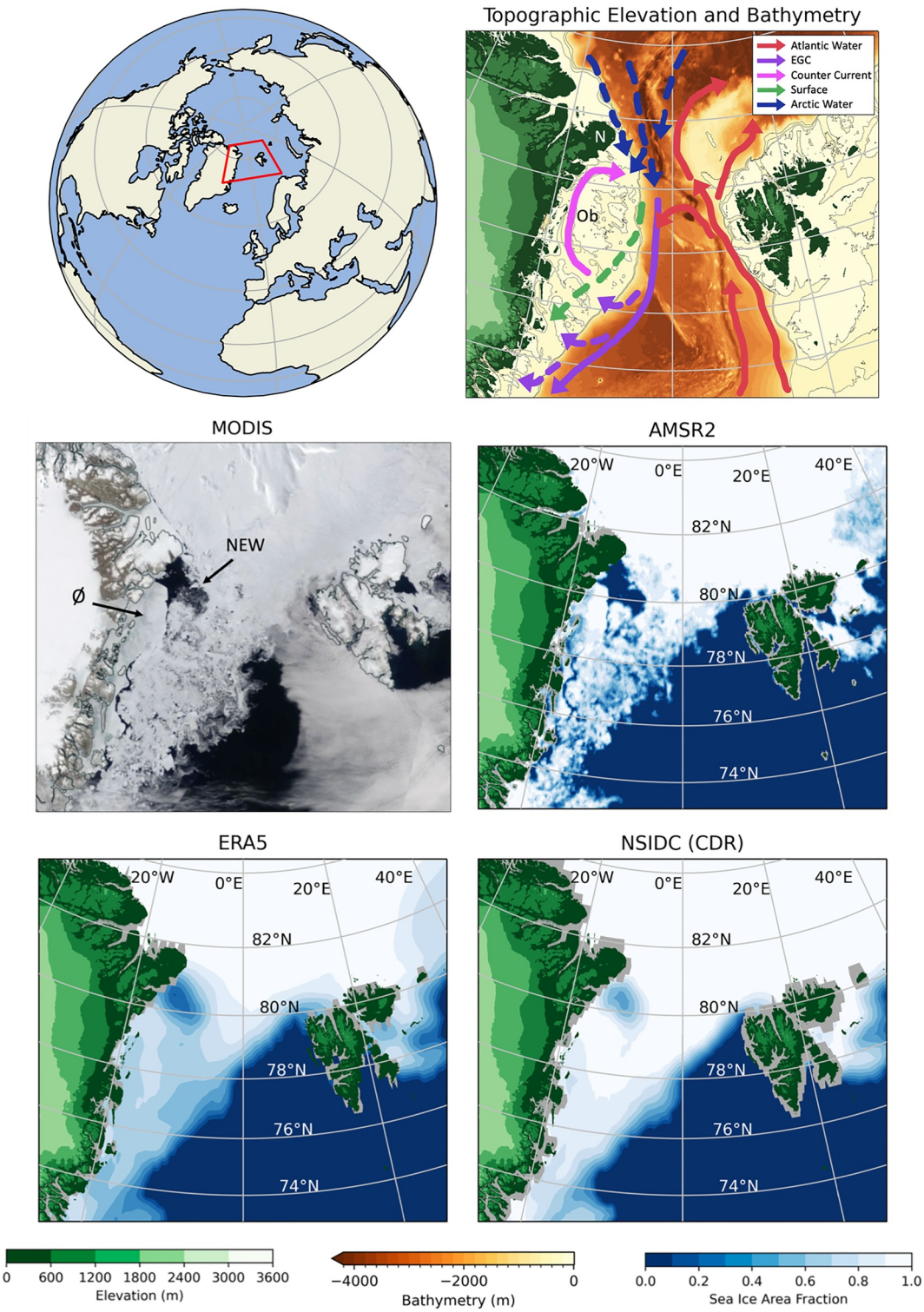

Figure 1. The region of interest has complex bathymetry and ocean circulation as illustrated in the upper right panel which shows the GEBCO product for bathymetry and the STRM30 product for topographic elevation. The major known and hypothesized currents are represented schematically by the solid and dashed arrows respectively. The Ob Bank (Ob) and Nørdoststrundingen headland (N) are labeled. Additionally, we show the Northeast Water (NEW) Polynya on 21 June 2020 as visualized by NASA's MODIS (Moderate Resolution Imaging Spectroradiometer) instrument (center left panel), and the equivalent daily sea-ice product from AMSR2, ERA5 and National Snow and Ice Data Center (NSIDC) (center right, lower left and lower right panels). The STRM30 topography is also shown here. The polynya (NEW) and Norske Øer Ice Barrier (Ø) are indicated in the MODIS Satellite image. The region of interest is highlighted in red in the upper left panel.

activity and to support many Arctic species, including the critically endangered Spitsbergen stock of bowhead whale (Speer et al., 2017). The polynya is also the most important calving area for the northeast Greenland stock of walrus, and supports the largest known breeding colony of ivory gulls in Greenland (Speer et al., 2017). Given its importance for marine wildlife, many of the published studies on this polynya focus on its ecological characteristics rather than the environmental physics of the region. However, polynyas of this size and frequency can have significant impacts on local atmospheric dynamics, oceanic processes and the climate system more broadly (Barber & Massom, 2007). For example, polynyas can drive dense-water formation (e.g., Martin & Cavalieri, 1989; Ohshima et al., 2016), act as carbon sinks (e.g., Yager et al., 1995) and increase rates of cloud formation (e.g., Dare & Atkinson, 2000; Monroe et al., 2021; Morales Maqueda et al., 2004). Polynyas can have a significant effect on atmospheric mesoscale motion, by releasing heat from the ocean to the atmosphere at a rate of one to two orders of magnitude greater than occurs with thick ice cover, leading to convective cells or circulation features (Kottmeier & Engelbart, 1992; Maykut, 1982). Additionally, polynyas are crucial to the production of new sea-ice, often being to referred to as "sea-ice factories." The NEW Polynya is considered a relatively productive polynya for its size and has been estimated to produce approximately 136 km^3 of sea-ice each year (Iwamoto et al., 2014; Tamura & Ohshima, 2011). As sea-ice declines throughout the Arctic, indigenous communities are facing challenges to their traditional ways of life, while new opportunities open for shipping, fishing, tourism and natural resource extraction (Meier et al., 2014). With the rising presence of human activity in this region, the requirement for improved understanding and accurate monitoring of the atmosphere, ocean and sea-ice continues to grow.

Polynyas are usually classified as being driven by either latent or sensible heat processes. Latent heat polynyas form due to divergent ice motion as a result of the prevailing winds and/or ocean currents, whereas, sensible heat polynyas develop due to high surface ocean heat fluxes (e.g., Hirano et al., 2014; Morales Maqueda et al., 2004). The NEW Polynya demonstrates elements of both latent and sensible heat polynya processes (Barber & Massom, 2007), and thus is not easily classified according to the traditional characteristics of polynya categorization. In previous studies (e.g., Barber & Massom, 2007; Budéus & Schneider, 1995; Smith & Barber, 2007) the exact driving mechanisms for the formation of the NEW Polynya are ambiguous and explanations are largely speculative, mostly due to a lack of in situ observational data. The intricate oceanography in this region adds to the uncertainty. The bathymetry of the Greenland Sea and Fram Strait varies dramatically, with depths of over 5,000 m recorded in the deepest area to the west of Svalbard, known as the Molloy Deep, and in contrast, depths of just 200 m seen on the East Greenland continental shelf, known as the Ob Bank (Klenke & Schenke, 2002) (Figure 1). There is also a complex pattern of ocean currents, with various structures and properties, such as the West Spitsbergen Current (e.g., Moore et al., 2022), East Greenland Current (e.g., Holliday et al., 2007; Jeansson et al., 2008; Sutherland & Pickart, 2008) and Return Atlantic Current (e.g., Rudels & Friedrich, 2000; Schauer et al., 2004). Additionally, there are more recently identified features on the continental shelf, such as the North East Greenland Coastal Counter Current (Figure 1) which is thought to show a seasonal cycle of variability, with northward flow in summer and southward flow in winter (Karpouzoglou et al., 2023). Many of these oceanic flow features are important in forming the high latitude branches of the global thermohaline circulation system (e.g., Moore et al., 2022; Weijer et al., 2022). Furthermore, the large annual variability of freshwater influx from the Greenland Ice Sheet plays a role in the oceanic structure here (Sejr et al., 2017) and further complicates the coupling between the atmosphere and the ocean.

Although having been identified as early as 1935 (Koch, 1935), given its remote nature, the NEW Polynya was not easily observed for some time. Following a research cruise in 1993, there were several publications. For example, Budéus and Schneider (1995) focus on the hydrography of the polynya, using observational data from buoys, and conclude that its formation is not driven by processes typical of either a latent heat nor a sensible heat polynya. The high interannual variability of the NEW polynya has been referred to in several studies (Barber & Massom, 2007; Böhm et al., 1997; Deming, 1993), although further details, and a more recent update, would be beneficial. While the interaction of the northward coastal current with the Norske Øer Ice Barrier to the west is thought to be a major factor in creating the NEW Polynya, it cannot be termed a pure latent heat polynya, as a balance between freezing rate and ice export is not present (Budéus & Schneider, 1995); while it cannot be a pure sensible heat polynya as melt alone is not the driver (Barber & Massom, 2007). Additionally, the grounding of deep-draft icebergs can prevent ice advection into the polynya from the north, leading to its expansion (Barber & Massom, 2007). At present, the dominant driving mechanisms of the NEW Polynya remain unclear.

Despite its importance for the wider Arctic and proximity to the fast changing ice edge, little is known of the physical processes leading to the development, maintenance and variability of the NEW Polynya. The spatial and temporal variability of its annual formation and closure are also undocumented. With significant improvements in both satellite measurements and reanalysis products in recent years, there is now the opportunity to comprehensively characterize this polynya. This study aims to.

- Develop a climatology of the NEW Polynya; documenting where and when it develops and characterizing its variability.
- Determine what drives the formation, maintenance and variability of the NEW Polynya; for example, is it largely a result of atmospheric or oceanic forcing?
- Determine how the NEW Polynya has changed over the last few decades.
- Discuss how the NEW Polynya might continue to evolve under the changing climate and what implications this might have for other aspects of the Arctic environment.

2. Data

We use the European Center for Medium-Range Weather Forecasts (ECMWF) reanalysis products ERA5 and ORAS5 to examine near surface atmospheric and oceanic variables in the vicinity of the NEW Polynya.

ERA5 is the fifth generation ECMWF meteorological reanalysis (Hersbach et al., 2020). It has global coverage on a horizontal grid of approximately 31 km and has 137 vertical levels. It uses the Integrated Forecasting System (IFS Cycle 41r2). We use daily and monthly mean output from 1980 to 2022, so starting when satellite observations of sea-ice area became routine. The evolution of sea-ice cover in ERA5 is based on a number of products over different periods of time (Hersbach et al., 2020). The UK MetOffice's Operational Sea-surface Temperature and sea-ice Analysis (OSTIA) data set is used from September 2007 to present, and this uses the EUMETSAT Ocean and sea-ice Satellite Applications Facility (OSI-SAF) 401 data set for sea-ice concentration (Donlon et al., 2012). OSTIA provides daily updated sea surface temperature and sea-ice fields, primarily sourced from infra-red and microwave satellite observations, with a horizontal resolution of approximately 0.05° (Eastwood et al., 2014; Good et al., 2020; Hersbach et al., 2020). Prior to this, between January 1979 and August 2007, the Met Office Hadley Center HadISST2 sea-ice product was used, which had a horizontal grid of 1/4° (Titchner & Rayner, 2014) and was primarily derived from the Global Sea Ice Concentration daily data record (OSI-409a) produced by EUMETSAT's OSI-SAF. ERA5 generally compares well to surface-layer meteorological observations in the Nordic Seas and in the vicinity of the sea-ice edge (e.g., Renfrew et al., 2021), and has previously been used to study polynyas (e.g., Ding et al., 2020).

ORAS5 is ECMWF's OCEAN5 global eddy-permitting ocean-sea-ice ensemble reanalysis system. It estimates the state of the global ocean and comprises a Behind-Real-Time component, which provides an estimate of the historical ocean state from 1979 to near present-day, and a Real-Time component, that provides the latest ocean conditions (Zuo et al., 2019). ORAS5 has global coverage with a horizontal resolution of 1/4° and 75 depth levels. We use 43 years of monthly averages of potential temperature, ocean salinity and velocity components. OCEAN5 is based on the NEMO ocean model (version 3.4.1) coupled to the LIM2 sea-ice model (the Louvain-la-Neuve sea-ice model version 2), in global configuration ORCA025. L75 (Zuo et al., 2019). Observations are assimilated through the NEMOVAR data assimilation system. This ocean reanalysis product was partly chosen to ensure consistency at the ocean surface, that is, for sea-surface temperature, sea-ice distribution and near-surface atmospheric variables.

Where possible, results from reanalyses are compared to observational data sets, such as oceanographic profiles (see Figures A3 and A4 in Appendix A). The ERA5 sea-ice is also compared to the University of Bremen AMSR (Advanced Scanning Microwave Radiometer) and the National Snow and Ice Data Center (NSIDC) Climate Data Record (CDR) products which are available from mid-2002 (Spreen et al., 2008) and late-1978 respectively (see Figure A1 in Appendix A).

The Bremen product uses AMSRE data between May 2002 and December 2011, and AMSR2 from May 2012 onwards (Ludwig et al., 2020). The NSIDC product is from Scanning Multichannel Microwave Radiometer (SMMR) instruments and Special Sensor Microwave/Imager and Special Sensor Microwave Imager/Sounder (SSM/I-SSMIS) passive microwave data. The CDR algorithm output is a rule-based combination of ice

concentration estimates from two well-established algorithms: the NASA Team algorithm (Cavalieri et al., 1984) and NASA Bootstrap algorithm (Comiso, 1986).

In general, there is good agreement across the sea-ice products, but the ERA5 and NSIDC products exhibit significantly more smoothing than the AMSR products, often overestimating sea-ice area fraction in the polynya region and the area of the marginal ice zone, which in reality has a more concise transition at the ice edge (e.g., Renfrew et al., 2021). This can be seen in Figure 1, for example, Although relying solely on reanalyses has its limitations, given the lack of available observational data sets for this region and the aims of this study, we argue that its use is appropriate, particularly for considering long-term trends, variability and forcing mechanisms.

3. Results

3.1. Climatological Overview of the Northeast Water Polynya

The NEW Polynya generally develops in mid-June and remains open until the beginning of late-September, with its maximum extent peaking in August. Figure 2 shows a seasonal mean climatology from 1980 to 2022 from ERA5 reanalysis products, with the sea-ice area fraction, mean-sea-level pressure (MSLP) and 10 m winds. It is clear that there is little variation in the MSLP and near-surface wind fields over the autumn, winter and spring seasons, with a consistent pressure gradient across Fram Strait; high MSLP to the northwest over Northeast Greenland and lower pressure to the southeast, driving a relatively strong northerly atmospheric flow across the open ocean waters of the Greenland Sea (e.g., Van Angelen et al., 2011). Although the position and shape of the sea-ice edge across Fram Strait is similar in these three seasons, there is some variation in the sea-ice cover, with a marginally lower area fraction in the vicinity of the NEW Polynya in spring and autumn, compared to winter. There is also lower sea-ice area fraction to the north and west of Svalbard in autumn than in winter and spring.

In summer the situation is quite different. The polynya is evident as an area of reduced sea-ice fraction near the coast of Northeast Greenland, with the Norske Øer land fast ice barrier to the west and the sea-ice edge to the southeast. There is almost no gradient in MSLP and consequently there is a collapse of the northerly flow regime seen in the other three seasons. Across the Greenland Sea the 10 m winds are weak and in some areas they are completely reversed in direction, with a southerly flow regime and increased directional divergence over the site of the NEW Polynya. Throughout the year there remains strong orographic winds in Northeast Greenland with the steep and complex terrain forcing numerous katabatic and barrier flows (Mattingly et al., 2023; Moore & Renfrew, 2005). These orographic flows show little seasonal variability (Figure 2). There appears to be an element of offshore flow near the NEW Polynya and the Norske Øer ice barrier which is more prominent in the summer months, when the northerly flow regime is weaker.

Figure 3 shows that the mean August ERA5 sea-ice area fraction differs significantly each year, with the location, structure and extent of the NEW Polynya changing dramatically. In the majority of years the NEW Polynya is coastal and seems to be located either to the south or east of the Nørdoststrundingen headland of Northeast Greenland. However, in some years it develops further offshore (e.g., in 1982, 2003, 2005, 2014, 2019, and 2022); while in other years, particularly where there has been a large northward retreat of the sea-ice edge, the polynya merges with the open ocean (e.g., in 2004, 2010, 2016, 2017, 2018, and 2021). The fact that this occurs more in recent years, suggests it is a feature of Arctic summertime sea-ice retreat. The significant interannual variability indicates that the driving mechanisms of the NEW Polynya are complex and changeable on an annual timescale.

Figure 4 (upper left panel) shows the annual frequency of 10 m winds in excess of 10 m s^{-1} for the same domain using monthly averages. The frequency is expressed as a percentage, calculated by taking the number of months where the monthly mean wind speed in the box exceeds 10 m s^{-1}, divided by the total number of months considered (516 for the annual period and 129 for the summer period), then multiplied by 100. As illustrated by the red shading there are strong winds relatively regularly in the location of the NEW Polynya, with an area of darker red (between 20% and 25%) to the east of Northeast Greenland. This correlation between a region of frequent high speed winds and the site of the NEW Polynya suggests a connection between the sea-ice distribution at the surface and the low-level wind speed. In summer, a similar area of relatively higher frequency of strong winds (6%–8%) is shown to the north of the location of the NEW Polynya, while much of the Fram Strait and East Greenland continental shelf region shows very low frequencies (<2%), see Figure 4 (lower left panel). This highlights the significantly reduced 10 m wind speeds during the summer months, compared to the rest of the year, particularly along the marginal ice zone.

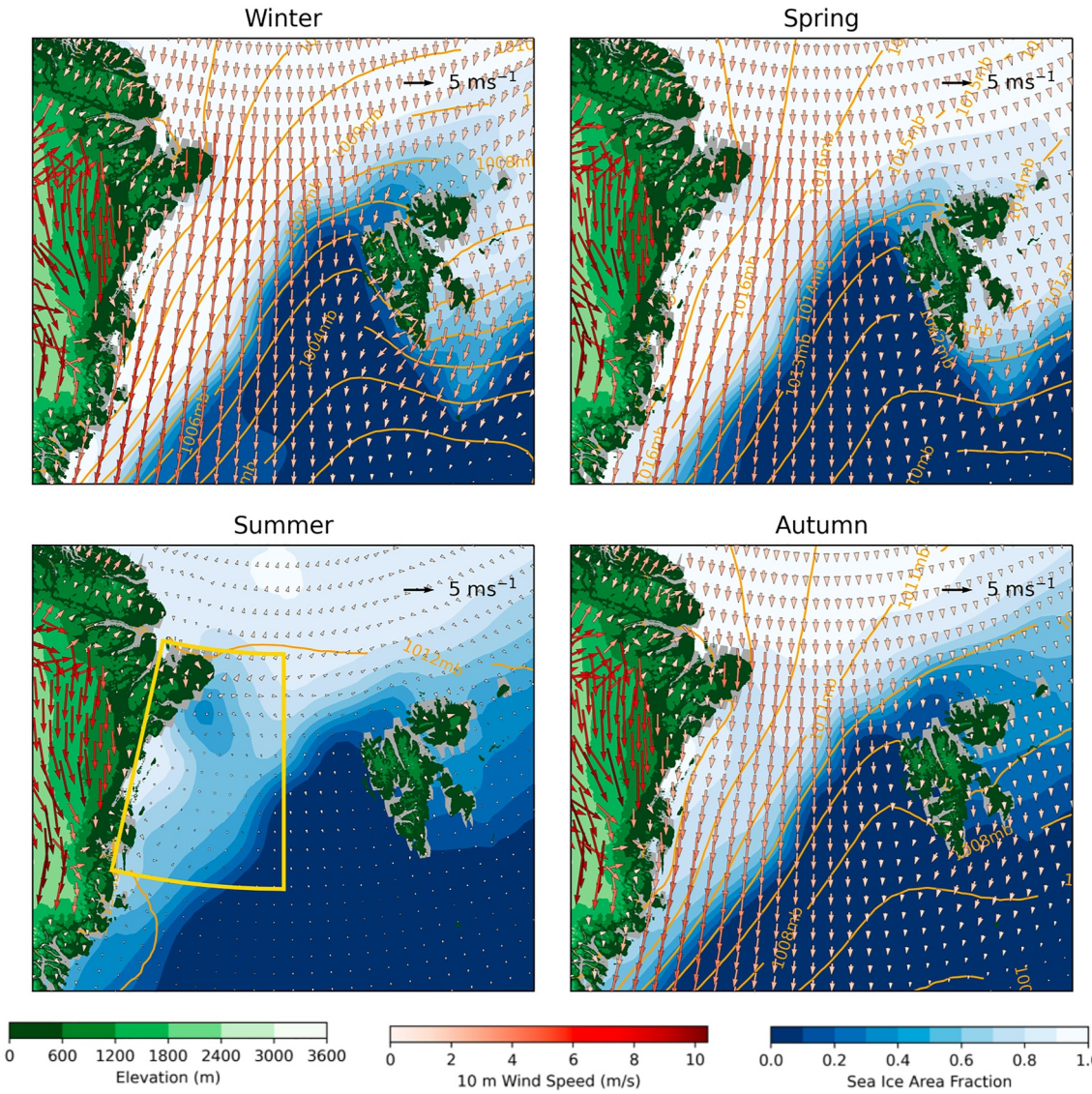

Figure 2. Mean Winter (December, January, February), Spring (March, April, May), Summer (June, July, August) and Autumn (September, October, November) climatology from 43 years of ERA5 products from 1980 to 2022 inclusively, showing sea-ice area fraction, 10 m winds and mean sea-level pressure contours (every millibar). The STRM30 topography is shown in green. The yellow box shows the area used for spatial averages over the Northeast Water Polynya.

Figure 4 also shows the directional constancy (DC). This is calculated using Equation 1 and monthly averaged 10 m zonal (u) and meridional (v) wind field components.

$$DC = \frac{\overline{u}^2 + \overline{v}^2}{\overline{u^2 + v^2}} \quad (1)$$

The DC is a useful diagnostic measure of persistence in the wind field with values of more than 0.85 only occurring in regions subject to strong katabatic flows or persistent jets (Harden et al., 2011; Moore & Renfrew, 2005). It is clear that there is relatively strong DC over much of Fram Strait compared to the open ocean further south. Above the NEW Polynya region there are values of approximately 0.5–0.6 in the same area as the higher frequency high wind speeds. Again, the co-location of these features implies persistent wind forcing of the sea-ice in the location of the NEW Polynya. The same plot for only the summer months of the year shows a reduction in this DC over much of the region, including the location of the NEW Polynya. Much of the Greenland Sea has a DC of less than 0.1, with only a small area of between 0.4 and 0.5 seen off the coast of the

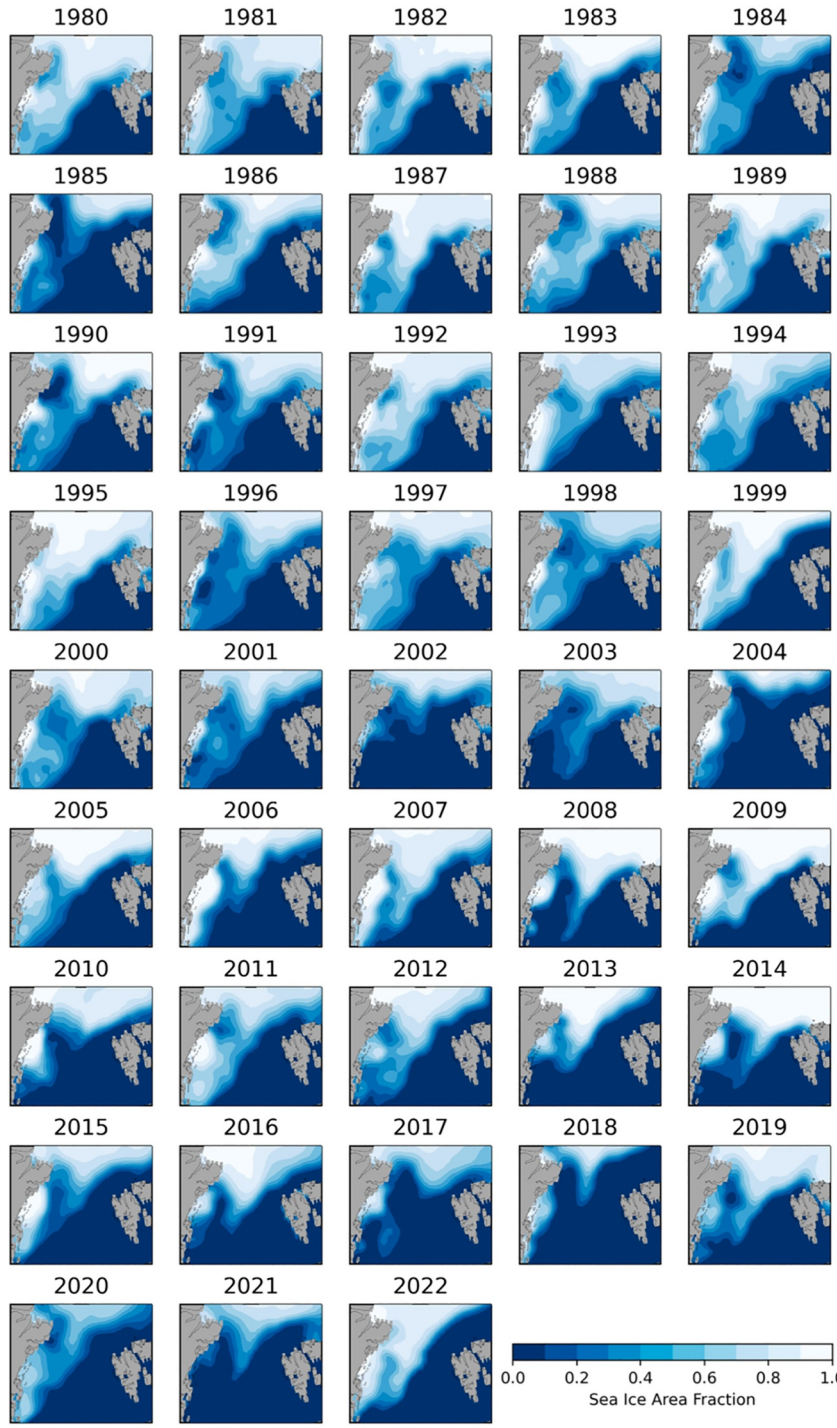

Figure 3. Interannual variability of the Northeast Water Polynya, illustrated with mean August sea-ice area fraction between 1980 and 2022 from ERA5.

Nørdoststrundingen headland just north of the polynya site. This highlights that there are much more variable near-surface winds in summer.

The annual cycle of the NEW Polynya region is summarized in Figures 5 and 6, using spatially averaged variables (averaged over the yellow box in Figure 2). Figure 5 illustrates the annual reduction in sea-ice from approximately mid-June to mid-October, with minima in August or September. This is mirrored by a noticeable increase in the

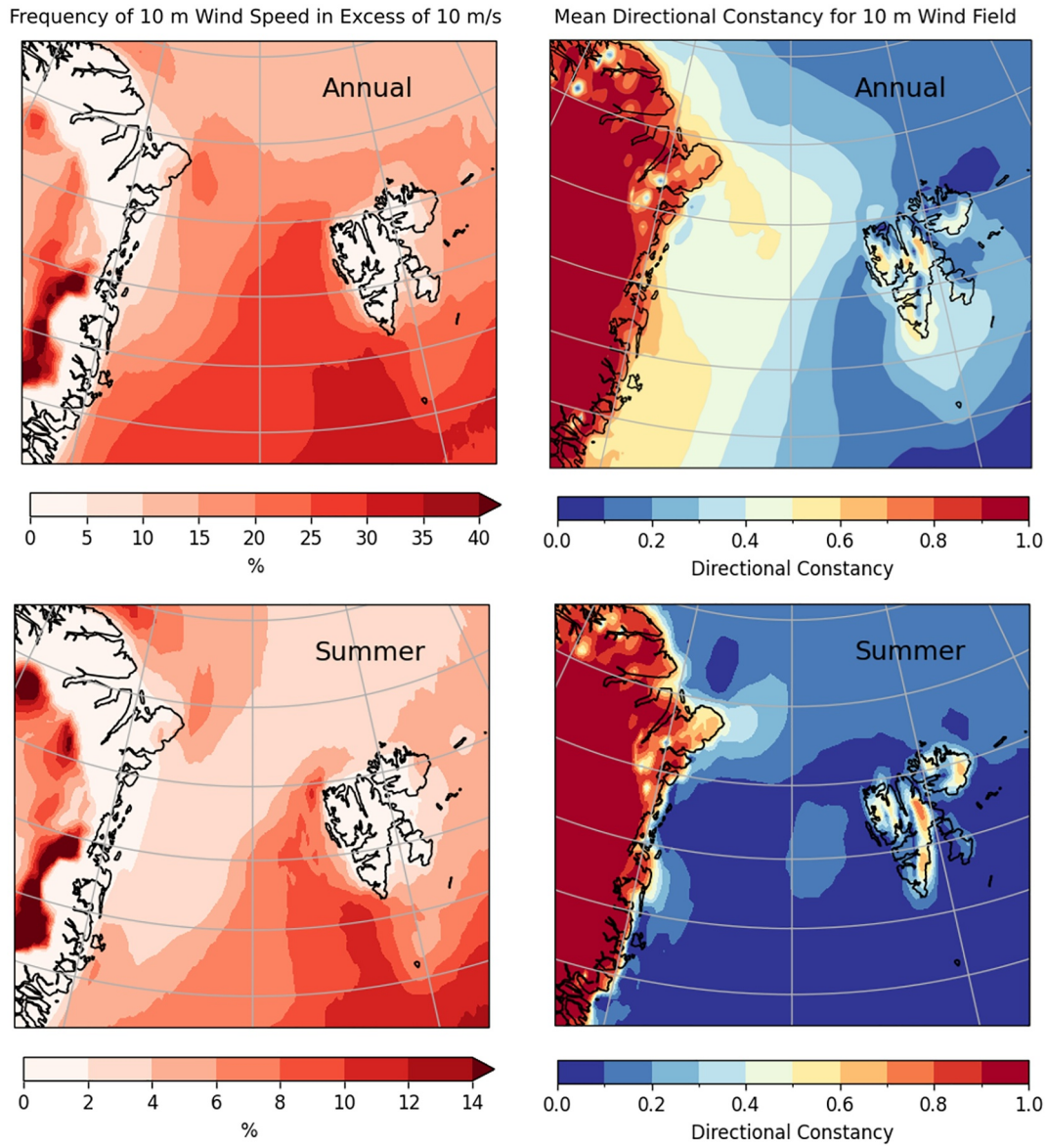

Figure 4. Frequency of 10 m winds in excess of 10 m s^{-1} (left column) and mean directional constancy (right column). The upper panels show results for all year and the lower panels show results for the summer months only (June, July, August).

2 m air temperature between April and October, with a wide peak over June and July. The lag between the annual 2 m air temperature increase and the sea-ice reduction implies that the atmosphere is warming before the summertime reduction in sea-ice, rather than the sea-ice reducing and then near-surface temperatures increasing. The 10 m meridional winds (positive values indicate a southerly flow, negative values indicate a northerly flow) show a cycle of annual variability, with stronger northerly flow in the winter months and a weaker, occasionally southerly, flow in the summer months.

The evolution in time (indicated by the blue to red lines in Figures 5 and 6) illustrates a general long-term trend of sea-ice decline and increasing temperatures in this region. There appears to be no significant long-term trend in the meridional wind speeds since 1980, although there is considerable variability throughout the year and between years.

To consider the variability of the ocean beneath the polynya, monthly averages of potential temperature and salinity from ORAS5 are shown at depths of approximately 0.5, 20 and 200 m (Figure 6). There is a clear annual cycle in the upper ocean with a near-surface potential temperature maximum and an ocean salinity minimum seen

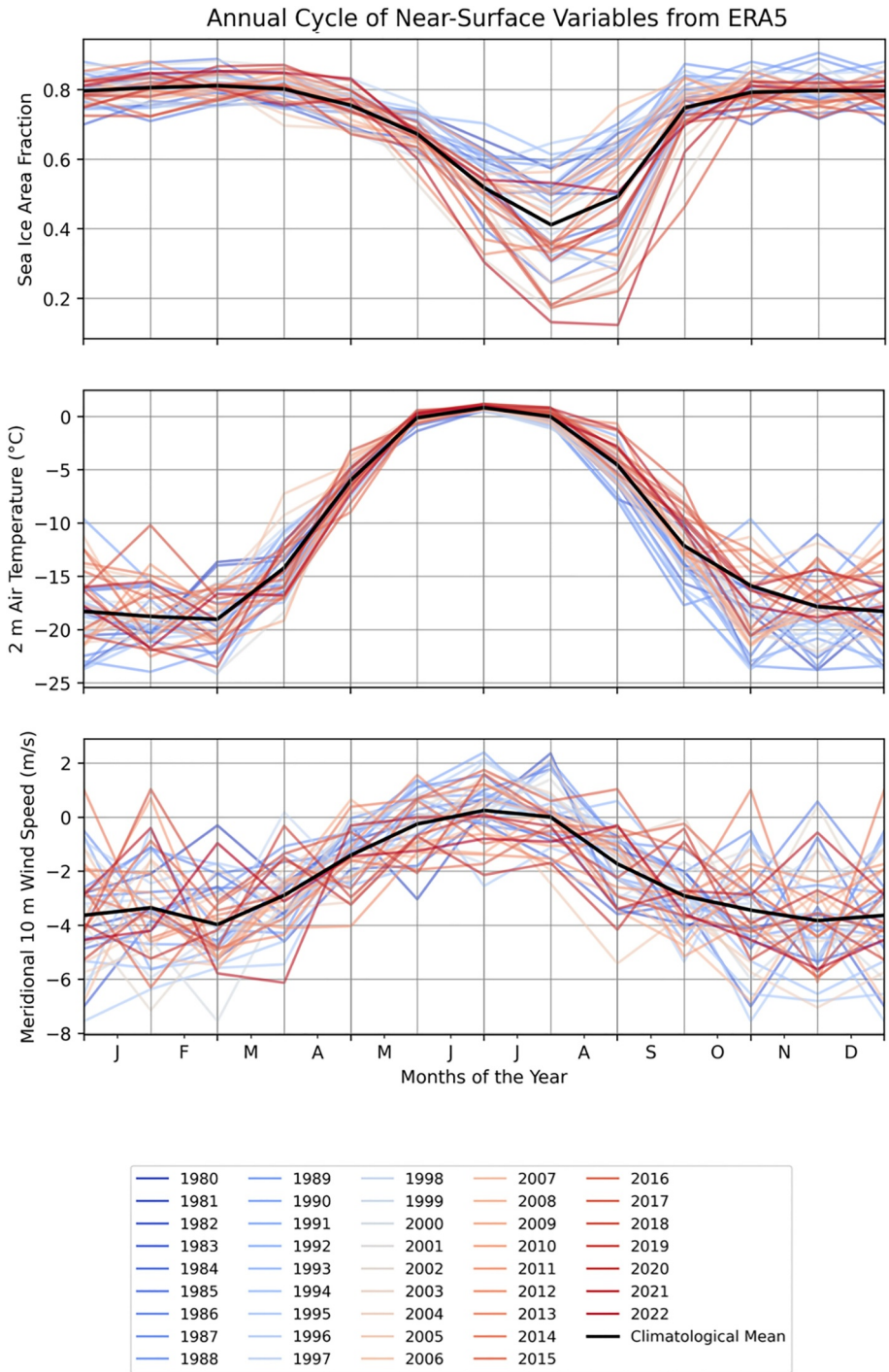

Figure 5. Annual cycle of monthly averaged sea-ice area fraction, 2 m temperature and 10 m meridional wind speed from ERA5 for each year between 1980 and 2022 (spatially averaged over the yellow box shown in Figure 2). The blue-to-red shading indicates the long-term trend. The black line represents the mean from all 43 years.

in approximately August and mid-July at 0.5 m and in August and October at 20 m, showing the influence of the surface variability on the ocean properties. The amplitude of the seasonal cycle decreases with increasing depth. At a depth of 200 m the annual cycle is less pronounced but still evident (more so with potential temperature than salinity). The fact that there is a lag in the cycle with depth implies that surface forcing of the ocean dominates over oceanic forcing of the surface. In spring, ice melts at the surface, freshening the uppermost layer of the water

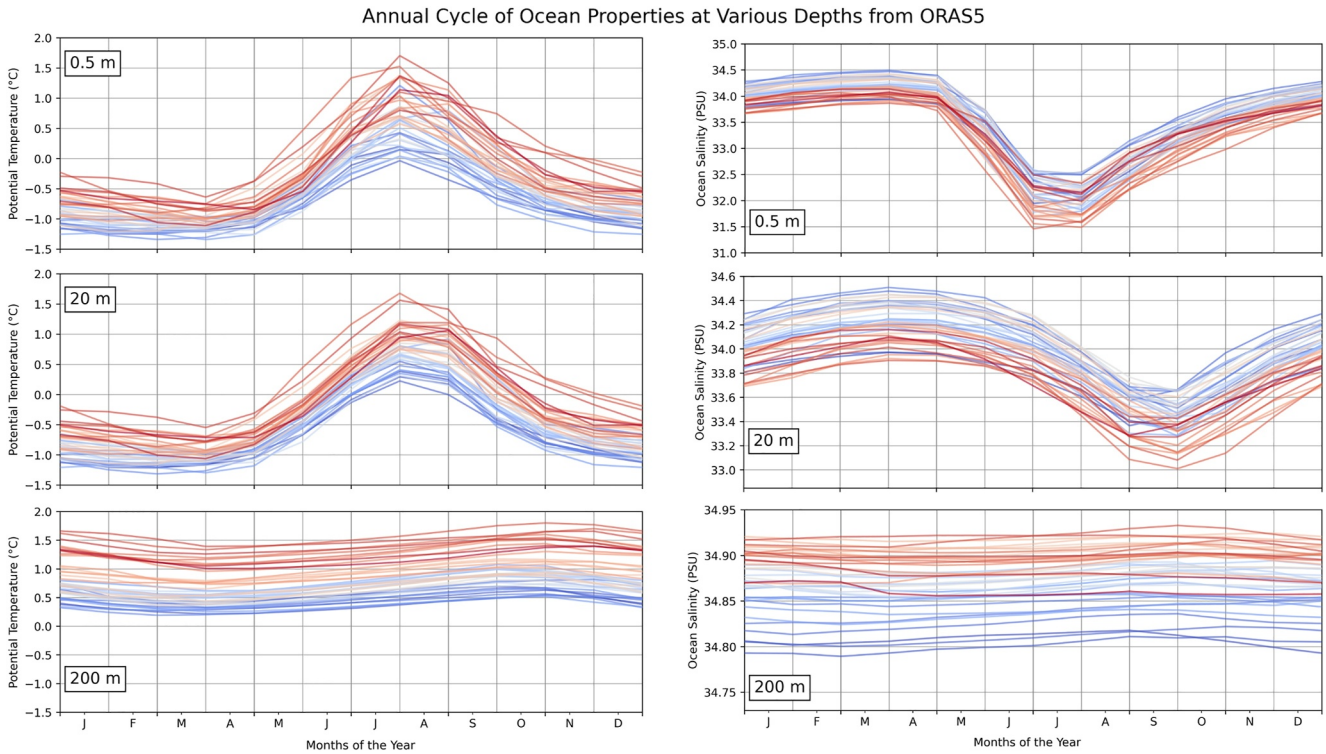

Figure 6. Annual cycle of potential temperature and ocean salinity at various depths from ORAS5 for each year between 1980 and 2022 (spatially averaged over the yellow box shown in Figure 2). The depths shown have been rounded for clarity. The true depth values are 0.5058, 19.43 and 199.80 m. The blue-to-red shading indicates the long-term trend, see legend in Figure 5.

column and exposing it to solar radiation and warmer air temperatures. As mixing occurs the relatively warm, fresh water is mixed down so the potential temperature increases and the salinity decreases. The lags in ocean warming and freshening with depth therefore imply surface forcing.

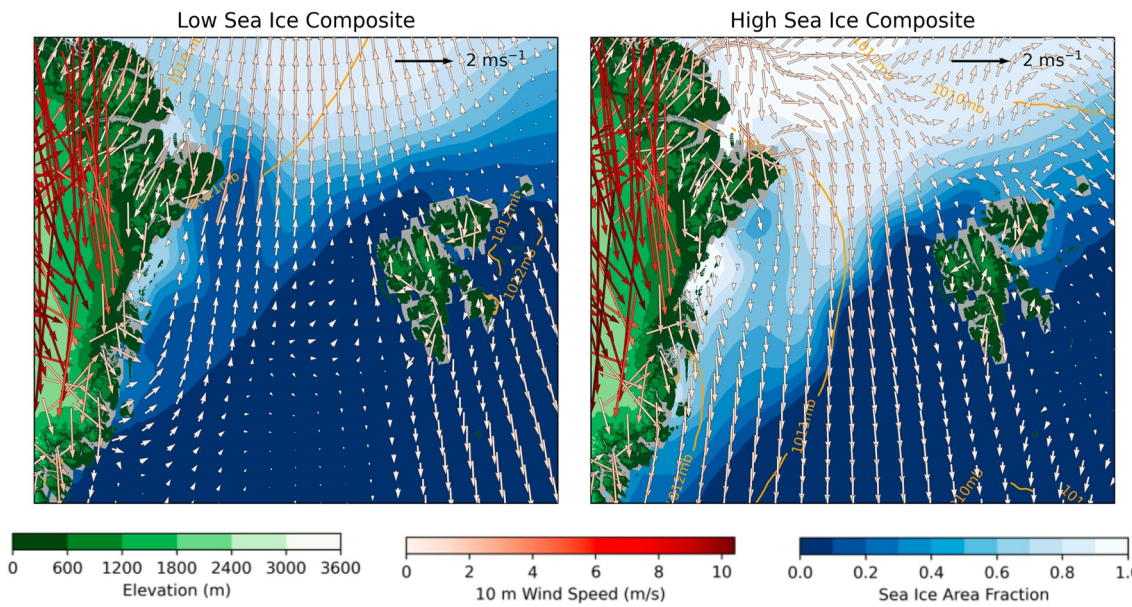

Figure 7. Composite mean August climatology from ERA5 using the 10 years with the highest and lowest sea-ice concentrations, respectively. The ERA5 sea-ice area fraction, 10 m winds and mean sea-level pressure fields are shown, and the STRM30 topography, as in Figure 2.

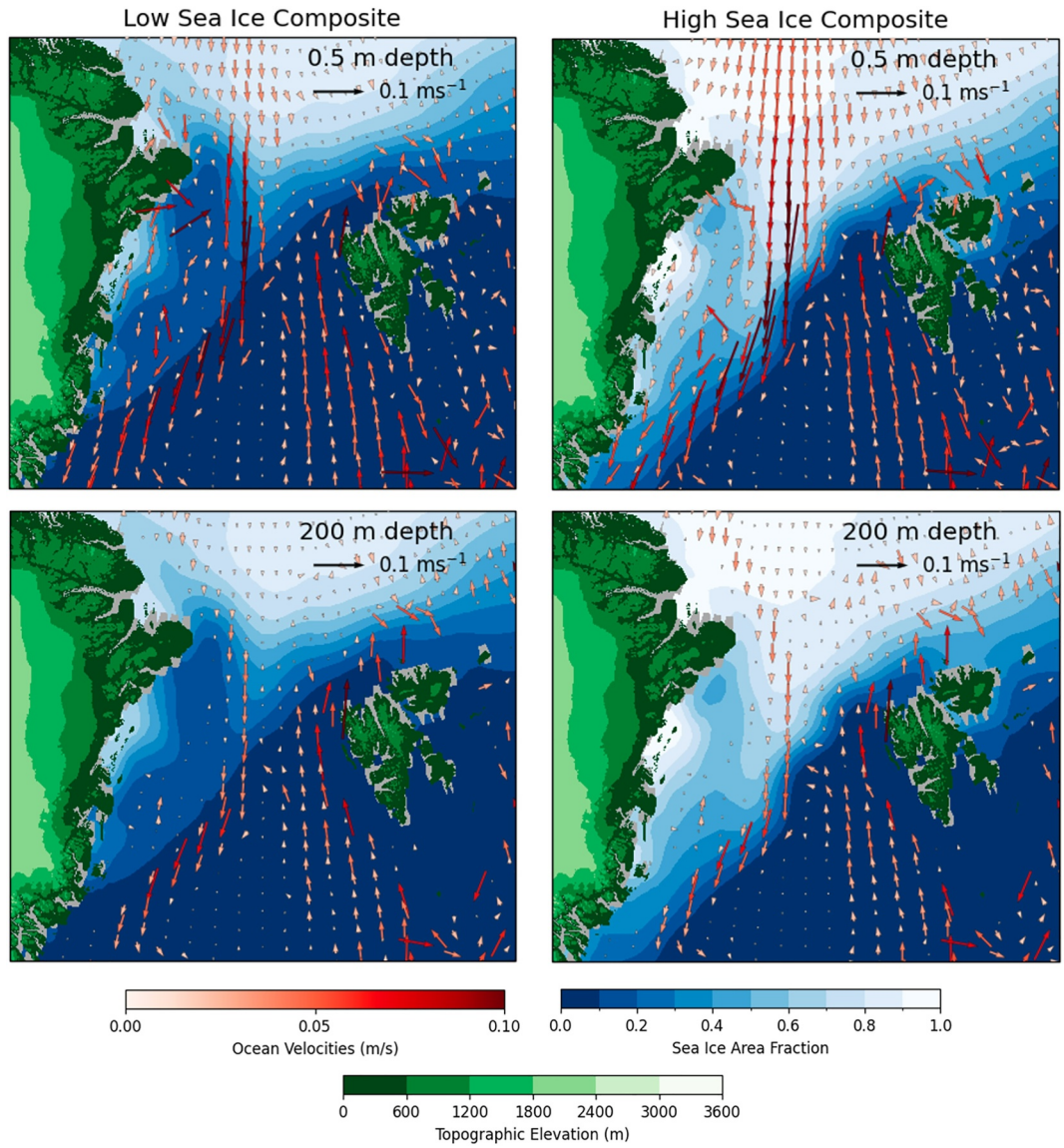

Figure 8. Composite mean August climatology using the 10 years with the highest and lowest sea-ice concentrations, respectively. The ERA5 sea-ice area fraction, the STRM30 topography and the ORAS5 ocean velocities at depths of approximately 0.5 m (upper row) and 200 m (lower row) are shown.

Over these four decades, a significant ocean warming is evident at all depths. In addition, there is a decrease in salinity in the upper two depth levels of 0.5 and 20 m, but an increase in salinity at 200 m depth. These changes are a result of anthropogenically forced warming and increased ice melt at the surface, combined with an increased flux of warmer and more saline Atlantic Water to this area via the West Spitsbergen Current (which is thought to be located at a depth of approximately 250 m in this region; Asbjørnsen et al., 2020; Tesi et al., 2021); they illustrate the "Atlantification of the Arctic" (Polyakov et al., 2017). The NEW Polynya sees both of these climatic drivers.

3.2. Composite Analysis Indicates Atmospheric Forcing and Oceanic Response

In order to further assess the mechanisms that lead to the annual formation and maintenance of the NEW Polynya, a composite analysis has been applied, based on the upper and lower quartile of minimum August sea-ice area fraction. From 43 years of daily ERA5 reanalysis products (see Figure A1 in Appendix A), the 10 Augusts with the highest and lowest mean sea-ice area fraction in the NEW Polynya region (yellow box shown in Figure 2)

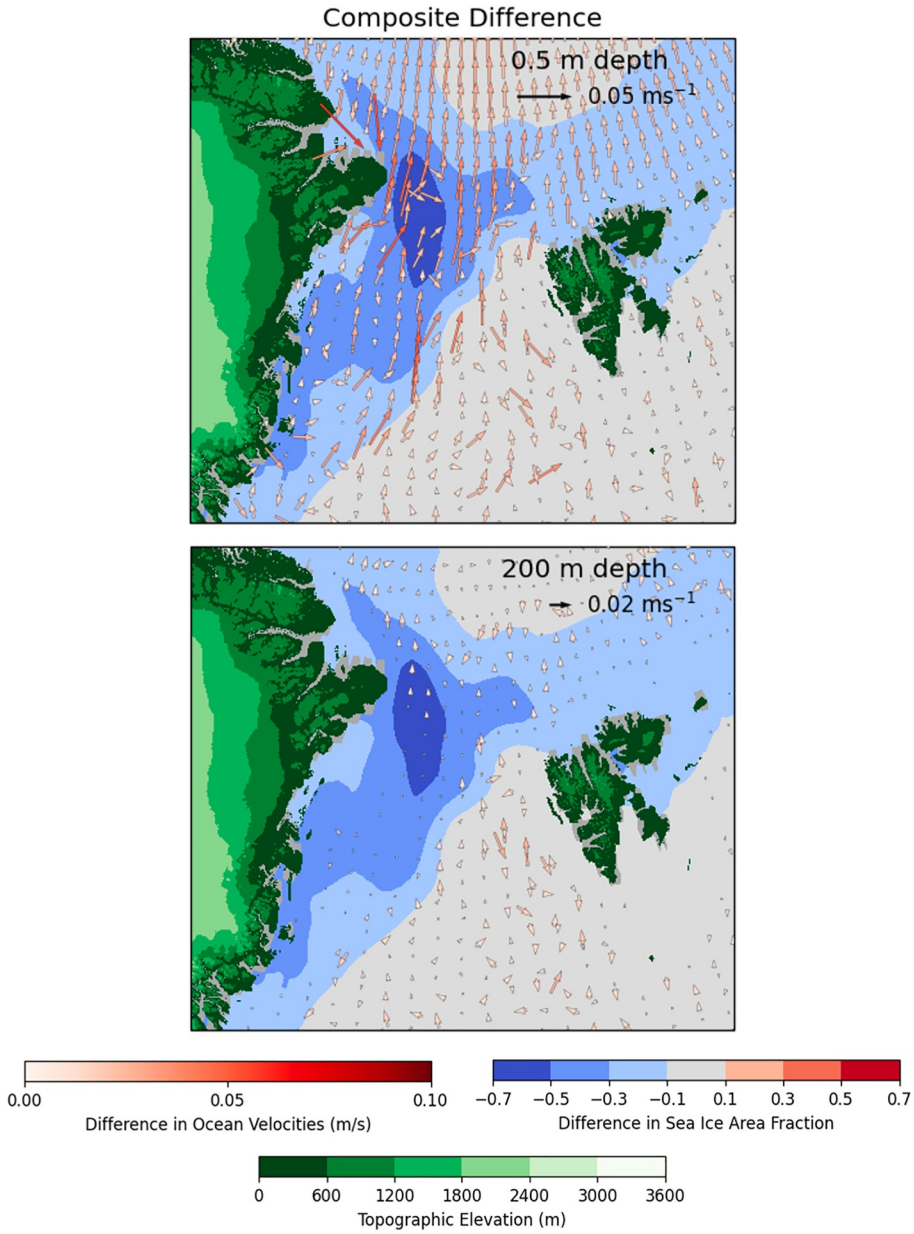

Figure 9. The difference between the low and high sea-ice composites shown in Figure 8 (low sea-ice years minus high sea-ice years), illustrating the difference in ORAS5 ocean velocities and ERA5 sea-ice area fraction.

were used to compile composite means (Figure 7). The 10 high sea-ice years are 1980, 1982, 1987, 1989, 1992, 1994, 1995, 1999, 2007, and 2009, and the 10 low sea-ice years are 1984, 1985, 1990, 1996, 2002, 2003, 2004, 2017, 2018, and 2020.

The size, shape and location of the polynya is different in each of the composite plots (Figure 7). The 10 m winds also show contrasting characteristics. In the high sea-ice composite, the wind field has uniform northerly flow of approximately 1 m s^{-1} over the Fram Strait region, while, in the low sea-ice composite the wind over the ocean is from the south at approximately 0.5 m s^{-1} and is more variable in direction. This stark contrast in the near-surface flow regime suggests a strong coupling between the 10 m wind field and the extent of the NEW Polynya at its maximum in August. It suggests the atmospheric flows are dictating the polynya's development. The MSLP field is weak in both composite climatologies.

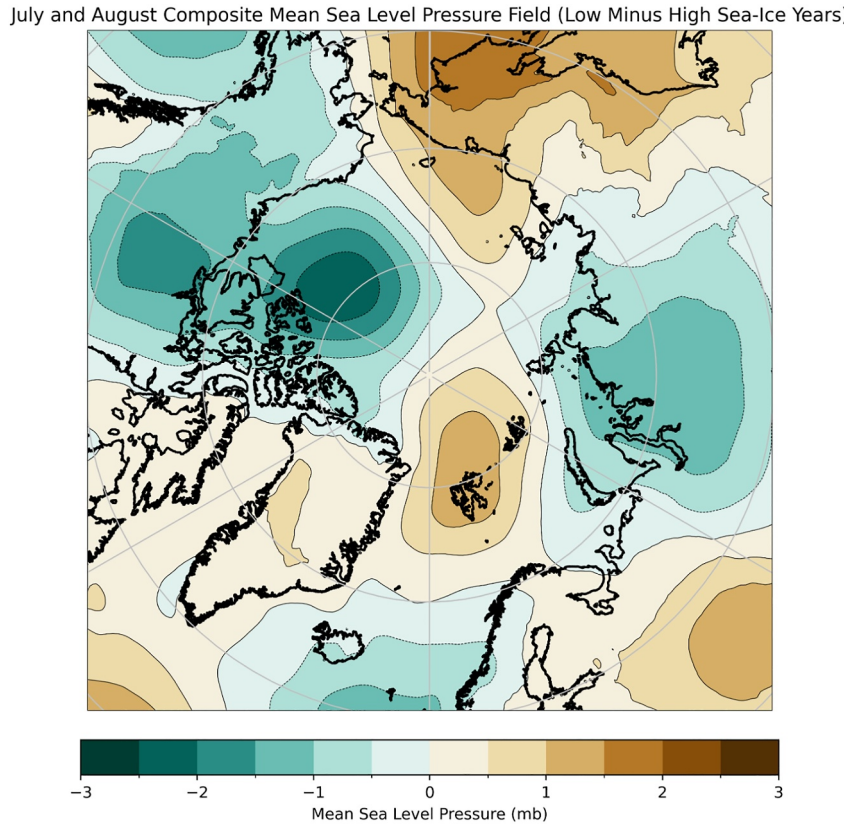

Figure 10. The difference between the low and high sea-ice composite pan-Arctic mean-sea-level pressure field for the months of July and August (low minus high sea-ice composite years).

To consider dynamical ocean forcing of the polynya we also look at ocean velocities in ORAS5 for the low and high sea-ice composites. Figure 8 shows the ERA5 sea-ice area fraction and the ORAS5 ocean velocities at depths of 0.5 and 200 m for each composite. The East Greenland Current and West Spitsbergen Current can be seen in all panels. The high sea-ice composite shows stronger ocean velocities over much of the region north of Fram Strait, flowing southwards into the East Greenland Current. This is particularly evident near the surface but can also be seen at 20 (not shown) and 200 m. At the site of the polynya, the low sea-ice composite shows stronger ocean velocities flowing eastward from the coast of Northeast Greenland, approximately along the pathway of the East Greenland Coastal Counter Current. The differences between the low and high sea-ice composites decrease with depth, indicating surface forcing, most likely by the near-surface winds in areas of reduced sea-ice cover. This is also illustrated in Figure 9 which shows the composite difference (low minus high sea-ice composite). There is little difference in the ocean velocities at 200 m depth and only small differences at 20 m (not shown). The clearest difference is at 0.5 m depth, where much of the region shows a stronger northward flow (or reduced southward flow) in the low sea-ice composite compared to the high sea-ice composite. This reflects results seen in Figure 7 which highlight a southerly wind regime for the low sea-ice composite in ERA5, and supports the hypothesis that atmospheric forcing largely controls the sea-ice distribution in the area of NEW Polynya.

In order to better understand the atmospheric forcing here, the MSLP field for the whole Arctic region for these composite months is considered. Figure 10 shows the difference between the mean July and August MSLP for the low and high sea-ice composites, calculated by taking the low sea-ice composite minus the high sea-ice composite, so the negative values (turquoise) indicate lower pressure and the positive values (brown) indicate higher pressure for years with lower summer sea-ice area fraction and a larger NEW Polynya extent. The pattern indicates enhanced southerly atmospheric flow over Fram Strait associated with an anomalous high over Svalbard. This pattern consistently appears for composites of various combinations of the summer months. For example, the difference between the low and high sea-ice composites for the mean June, July, and August sea-level pressure field looks very similar (not shown), suggesting a robustness to this result.

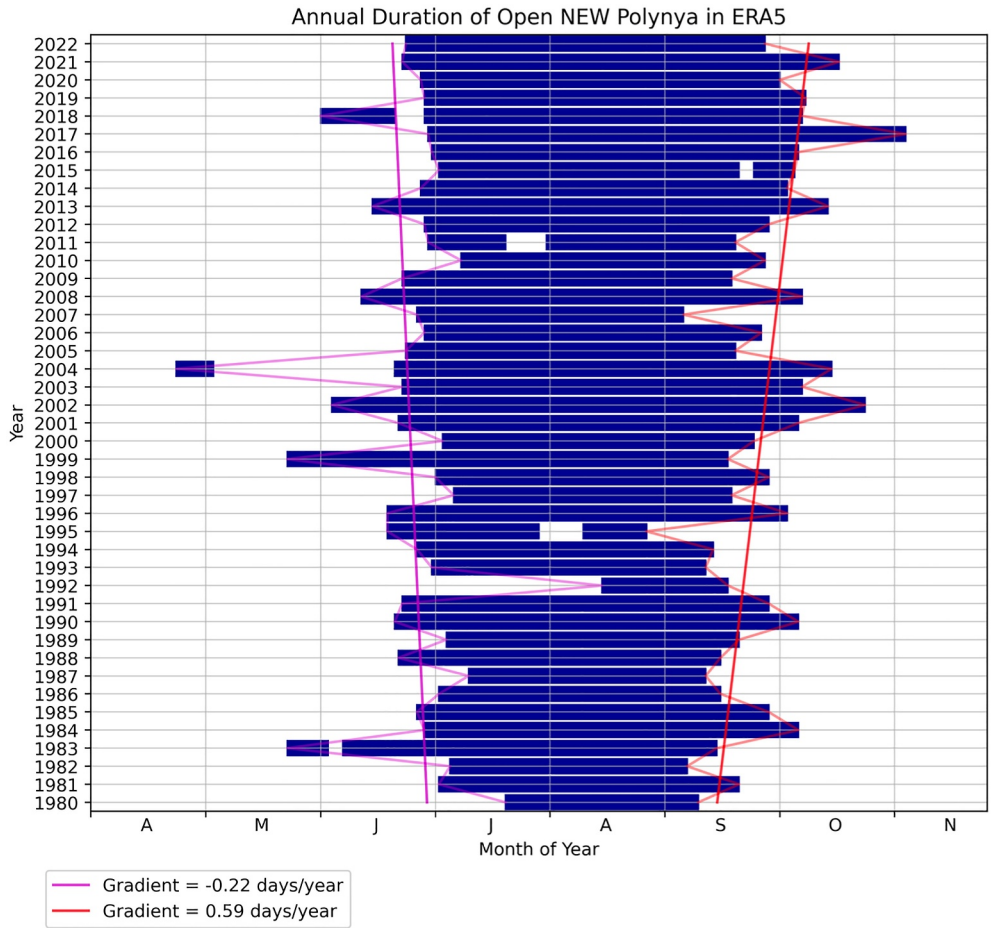

Figure 11. Annual timing of opening and closing of the Northeast Water (NEW) Polynya from ERA5 sea-ice area fraction. Here, a threshold value of 0.5 sea-ice area fraction (for the yellow box in Figure 2) and a threshold value of 10 consecutive days or more was used to designate the polynya as open. The long-term trends in the opening and closing of the polynya are shown in magenta and red, respectively. The closing trend is statistically significant at the 99% confidence level.

The emergence of this pattern suggests a relationship between the orientation of high and low sea-level pressure centers in the Arctic and the near-surface wind regime in the vicinity of the NEW Polynya. When there is higher pressure centered over Svalbard, and lower pressure the other side of the Arctic Basin, north of the Canadian coastline, a weak pressure gradient develops across the NEW Polynya region, with higher pressure to the east and lower pressure to the west. This is the reverse of the general mean climatology here, which usually drives northerly flow through the Greenland Sea and Fram Strait region (see Figure 2). The scenario during low sea-ice years (Figure 10), represents the collapse of this northerly flow regime and the subsequent development of a weak southerly flow associated with reduced sea-ice area fraction in the vicinity of the polynya. Therefore, it would seem that the interannual variability in the extent of the NEW Polynya is linked to the relative locations of two circulation systems over the Arctic Basin in the summer months. Note the magnitude of the differences in these MSLP systems is small, as is often the case for the summer months here.

3.3. The NEW Polynya Over the Last Four Decades

We now examine changes in the polynya over time. Figure 11 shows the period for which the NEW Polynya is classified as "open" for each year. This is determined from daily means of ERA5 sea-ice area fraction, the spatial average of which, for the box region shown in yellow in Figure 2, is used as a proxy for the polynya. A threshold value of 0.5 was chosen and whenever the daily mean sea-ice area fraction was less than this threshold value for 10 consecutive days or more, the NEW Polynya was categorized as being open. There is some sensitivity to this threshold value and different values should be used for different sea-ice products, however, sensitivity tests

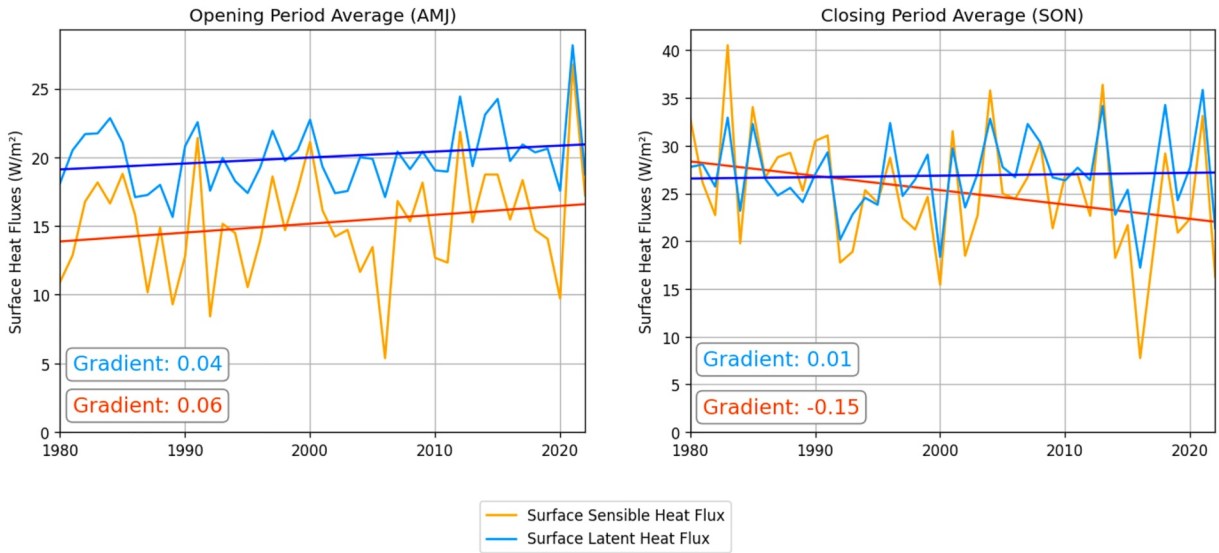

Figure 12. Trend in mean surface sensible and latent heat fluxes, between 1980 and 2022, spatially averaged over the yellow box shown in Figure 2, for the approximate polynya opening period (April, May, and June) and approximate closing period (September, October, and November). Data from ERA5. Note the vertical axis scale is different for each subplot. Positive values indicate an upwards flux (from ocean to atmosphere).

suggest that the climatological trends are qualitatively similar. Equivalent results from the AMSR and NSIDC sea-ice products are shown in Appendix A (see Figure A2).

Generally, the polynya opens at the beginning of July and closes in mid-September, remaining open for typically 10 weeks each summer. However, this appears to have changed over the last 43 years. There is a clear trend in the timings of the annual opening and closing of the polynya, with it generally opening earlier and closing later each year. The opening trend line marks a shift in the annual formation from approximately late-June in the early 1980s to approximately mid-June in more recent years. This is mirrored by the closing trend line, with the approximate date of closure shifting from mid-September in the 1980s to early October in more recent years. The closure trend line (0.59 days per year) is statistically significant with a p-value of less than 0.001. A similar result is found in other sea-ice products (Figure A2) indicating a robustness to this result. Consequently, the annual duration of the polynya is typically now approximately 14 weeks.

This result provides some of the first tangible evidence to support predictions from earlier studies that ice-edge polynyas in the Arctic are likely to transition into large marginal ice zones as the climate continues to change (Barber & Massom, 2007), before disappearing, possibly forever. For the first 20 years of the study period, the trend in ERA5 sea-ice area fraction for the NEW Polynya region is -0.02×10^{-4} per month, whereas the trend for the last 20 years is -1.8×10^{-4} per month, highlighting a shift at the turn of the millennium, which has also been highlighted in previous studies (e.g., Döscher et al., 2014). It is clear that the annually recurring and stable nature of the NEW Polynya seen in the last two decades of the previous century is now in the past and that due to increased Arctic warming, as a result of anthropogenic forcing, this important polynya could soon vanish. This could have significant impacts for local wildlife and people, and the interactions between the atmosphere and the ocean.

As the variability of the annual cycle at the surface decreases, and the polynya is open longer each year, the turbulent surface heat fluxes will also be affected. Figure 12 shows the ERA5 mean surface sensible and latent heat fluxes in the NEW Polynya region between 1980 and 2022, for the approximate opening and closing periods, which here are taken as the months April, May, June, and September, October, November respectively. Note that for all fluxes we use positive values to indicate an upwards flux, from ocean to atmosphere, and negative values to indicate a downwards flux, from atmosphere to ocean.

There is a trend of increasing surface fluxes in the opening period. The mean surface sensible heat flux increases from approximately 14 to 17 W m^{-2}, and the mean surface latent heat flux increases from approximately 19 to 21 W m^{-2}. This trend could be linked to sea-ice decline over this period, which results in a larger area of the ocean

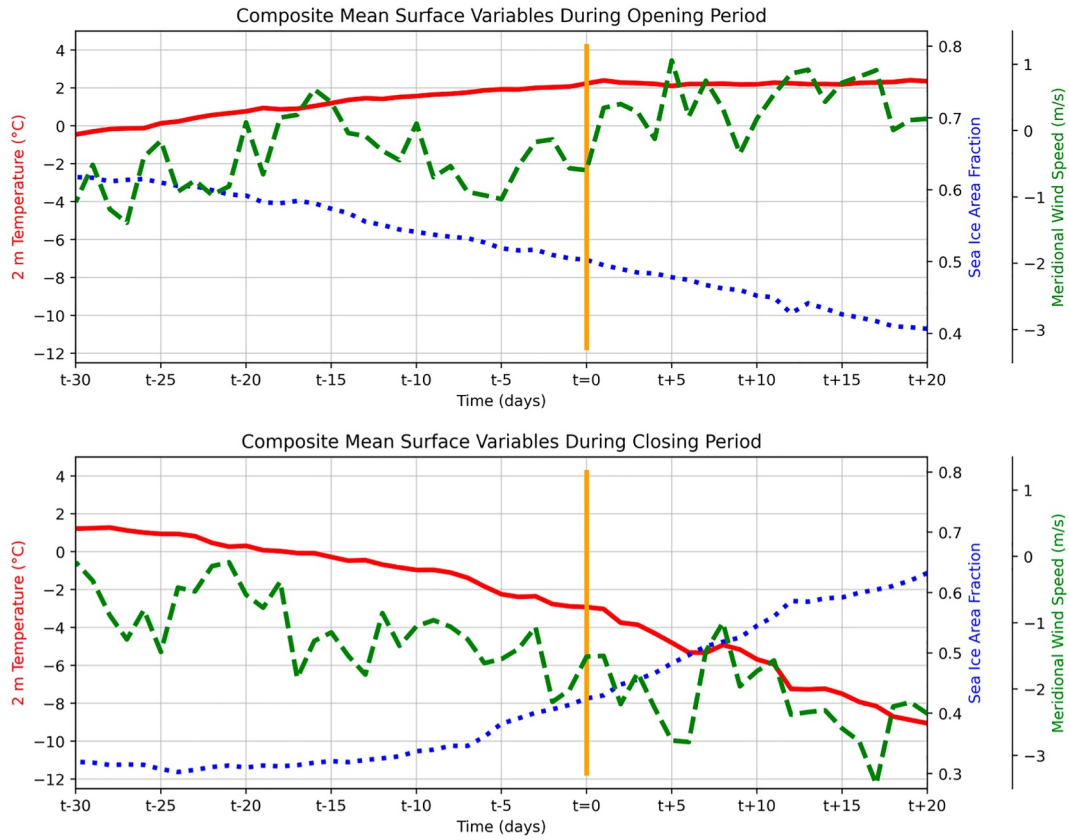

Figure 13. Time series showing the composite mean sea-ice area fraction (dotted blue), 2 m air temperature (solid red) and 10 m meridional wind speed (dashed green) from ERA5 for the yellow box shown in Figure 2 for the days in the month prior to the opening and closing of the polynya. Each daily mean is constructed from 43 years of data based on the timings of opening and closing identified previously and shown in Figure 11. In the upper panel, the time $t = 0$ represents the composite day of the polynya opening. In the lower panel, the time $t = 0$ represents the composite day of the polynya closing.

surface being exposed to the atmosphere and thus can lead to enhanced upwards surface fluxes (Moore et al., 2022). The trends indicate that the difference between the oceanic and near-surface atmospheric temperatures during the opening period is increasing, with the rate of warming of the ocean being larger than the rate of warming of the atmosphere. This is also illustrated in Figures 5 and 6 which show little variation in the spring and summer 2 m air temperature since 1980, but a significant warming of the ocean potential temperature at 0.5 m depth of approximately 1°C in spring and 1.5°C in summer. During this time of year, the ocean water is exposed to more solar radiation and warms more than the atmosphere, so as sea-ice declines in this region, the surface albedo decreases and the rate of warming increases and thus, so too does the surface sensible heat flux. The opening period trends for the surface sensible and latent heat fluxes have p-values of 0.18 and 0.14 respectively and thus are only of near-marginal statistical significance.

For the closing period, there is a negligible change in the latent heat flux since 1980 (less than 1 W m^{-2}) and the sensible heat flux shows a decrease from approximately 28 to 22 W m^{-2}. This indicates that the difference between the near-surface oceanic temperature and the near-surface atmospheric temperature is decreasing in the closing period with the rate of warming of the ocean being smaller than the rate of warming of the atmosphere. In Figures 5 and 6, there is an increase in the autumn 2 m air temperature of approximately 10°C since 1980 and a less pronounced increase of approximately 1°C in the ocean potential temperature at 0.5 m depth. The fact that there is an increase in the near-surface air temperature in autumn is linked to the decline in sea-ice in this region and the fact that the polynya is closing later during this period. The negative trend in surface sensible heat flux for the closing period suggests a link to the trend of the annual closure of the NEW Polynya; the formation of new ice increases the surface latent heat flux and with this now occurring later in the year, there is a negative trend for this transition period. The closing trend for the surface sensible heat flux is statistically significant with a p-value of 0.05.

Our results indicate a strong coupling between the sea-ice variability in the NEW Polynya region and the near-surface atmospheric flow regime. To investigate further, composite data sets for the periods around the opening and closing have been constructed using ERA5 daily variables (Figure 13). In the upper panel, prior to the opening of the polynya (which is marked at 50% sea-ice area fraction), there is steady sea-ice decline. This is associated with a small increase in 2 m air temperature of approximately 2° over the 30 day period. With temperatures hovering just above 0°C here, it appears that the atmosphere near the surface has already warmed before this composite 30-day period (in winter, 2 m air temperatures are approximately −20°C, see Figure 5). The 10 m meridional winds show a transition from a northerly to a southerly flow regime, and the southerly flow tends to strengthen in the days before the day of opening, although all wind speeds are relatively low.

In the lower panel, prior to the closing of the polynya, the composite air temperature is clearly decreasing dramatically, while the sea-ice area fraction is increasing. The simultaneity of these changes suggests a more synchronous transition in the autumn months, compared to that of springtime. The 10 m meridional winds are also showing a clear trend, changing from very weak speeds close to 0 m s^{-1} to northerly speeds of approximately 3 m s^{-1}. In summary, this time series composite indicates that dynamical forcing may play a larger factor in the formation of the NEW Polynya each spring, whereas thermodynamic processes are clearly more influential in its closure each autumn.

4. Conclusions

The NEW Polynya and local environment show significant annual variability in atmospheric and oceanic reanalysis products. During the summer, there are higher near-surface air and ocean temperatures and a weakening (and often complete reversal) of the low-level wind regime in the vicinity of the NEW Polynya, when the polynya is at its largest. There is also very little variation in the MSLP field across the domain during summer, in contrast to the rest of the year when there is generally a large east-to-west pressure gradient across Fram Strait and a strong northerly flow regime. The summertime sea-ice minimum coincides with a maximum in near-surface air temperature and a minimum in meridional wind speed. The ocean also shows a significant annual cycle with surface intensified higher temperatures and lower salinity in the summer months. There is a lag in the ocean cycle with depth. All-together, this points to the ocean responding to surface forcing as the NEW Polynya develops.

The NEW Polynya also shows significant spatial variability throughout the 43-year period considered. The structure of the sea-ice field in this region varies on seasonal, interannual and decadal timescales.

As for much of the Arctic, there has been a decline in sea-ice in the NEW Polynya region since the 1980s, and increasing atmospheric and oceanic temperatures (at all depths). There has also been a general freshening of the upper ocean layers with a trend of salinification at 200 m. These results indicate a significant environmental response to anthropogenic forcing and demonstrate there are already dramatic climatological changes in this region.

Composite analysis indicates that the peak summertime extent of the NEW Polynya is closely correlated to the near-surface atmospheric flow regime, with weak southerly flow associated with a lower sea-ice area fraction/larger polynya, and vice versa. This is attributed to the collapse of the pressure gradient across Fram Strait, which is related to the relative locations of high and low sea-level pressure centers over the Arctic, among other factors.

Ocean velocities reflect this variation in near-surface winds, with weaker southwards ocean velocities at 0.5 m depth over much of the region during summers with a larger polynya extent, compared to those with more sea-ice cover. The composite difference in ocean velocities is surface intensified, implying atmospheric forcing, particularly when the sea-ice area is reduced.

We conclude that the annual opening and closing of the NEW Polynya is closely coupled to the near-surface atmospheric flow regime, and although it is difficult to deduce the exact physical mechanisms driving the polynyas formation, it appears that both dynamic and thermodynamic processes play important roles. Wind forcing dominates the opening, while thermodynamic forcing dominates the closure. Both latent and sensible heat processes are at play here and thus, as concluded in previous studies, the NEW Polynya is not easily classified as simply a latent or sensible heat polynya.

In the real world there is no perfect way to separate atmospheric and oceanic drivers using only reanalysis products and observations, and it is difficult to quantify individual forcing mechanisms. Our composite analyses point to a primary role of atmospheric forcing, but numerous mechanisms are at play, on various timescales. Further exploration of these, using idealized modeling work, would be an interesting topic for a future study.

The NEW Polynya is clearly opening earlier and closing later in the year. Its duration is now typically 3 weeks longer than in the 1980s. This suggests a reduction in annual variability over time and a possible complete loss of the NEW Polynya as we know it today. In the future it is likely that, for many months of the year, this region will more closely resemble a broad marginal ice zone. This will impact the local environment and wildlife in many ways. For example, reduced sea-ice cover can result in increased summertime surface turbulent heat fluxes which cause a warmer atmosphere that in turn promotes sea-ice melt: a positive feedback loop. Meanwhile, the autumn period shows a decreasing trend in surface sensible heat flux due to very fast warming of the atmosphere and a longer period of ice melt (the annual initiation of ice formation is happening later in the year). These changes will have significant implications for both the atmosphere and ocean in this complex and rapidly changing environment.

Appendix A: Evaluation of Reanalysis Products

In order to evaluate the accuracy of the ECMWF reanalyzes in this region, ERA5 and ORAS5 output was compared to other data sets where available. Sea-ice products from AMSR and NSIDC generally show a good comparison to ERA5 sea-ice, both spatially and temporally, although the magnitude of the sea-ice area fraction is often different. Figure A1 shows the annual cycle of variability for the daily sea-ice area fraction in ERA5, NSIDC, and AMSR for the NEW Polynya region. Each year is shown with color shading from blue in 1980 to red in 2022. Note that the AMSR sea-ice product is only available from mid-2002 onwards.

Figure A1 illustrates a good correlation across the products. When looking at spatial maps, there tends to be more smoothing in the ERA5 and NSIDC sea-ice compared to AMSR, which generally shows sharper transitions at the sea-ice edge (see Figure 1).

For comparison to Figure 11, we have also constructed a plot for the open period of the polynya using the AMSR and NSIDC sea-ice products. Here a threshold value of 0.75 was used to classify the polynya as open, a different value to ERA5, in order to account for the general shift in the magnitude of the sea-ice area fraction seen in the different products. The results are similar to that seen in Figure 11 with a trend in the polynya opening earlier and closing later in the year. For the AMSR product, the trend of the closing period is statistically significant with a p-value of less than 0.001, suggesting a robustness to this result. For the NSIDC product, it is only the opening trend that is statistically significant.

To assess the quality of ORAS5 data (Zuo et al., 2019), comparisons to summertime observational conductivity, temperature and depth and expendable bathythermograph casts have been made where possible. Figures A3 and A4 show some examples of temperature and salinity profiles respectively, with inset maps to show the locations of the casts. The nearest ORAS5 equivalent has been plotted for each cast profile. Although there is often a fair agreement in the temperature profiles, the reanalysis tends to underestimate temperature near the surface and overestimate it beneath approximately 50 m depth. The fit appears poorer for the salinity profiles, where ORAS5 overestimates salinity throughout the water column. The ORAS5 product clearly has limitations in its representation of the ocean in this region. There is a relative paucity of observations to assimilate and point comparisons could be affected by unresolved variability. However, as used in this study, with a focus on long-term trends, variability and diagnosing forcing mechanisms, we would argue that its use is reasonable.

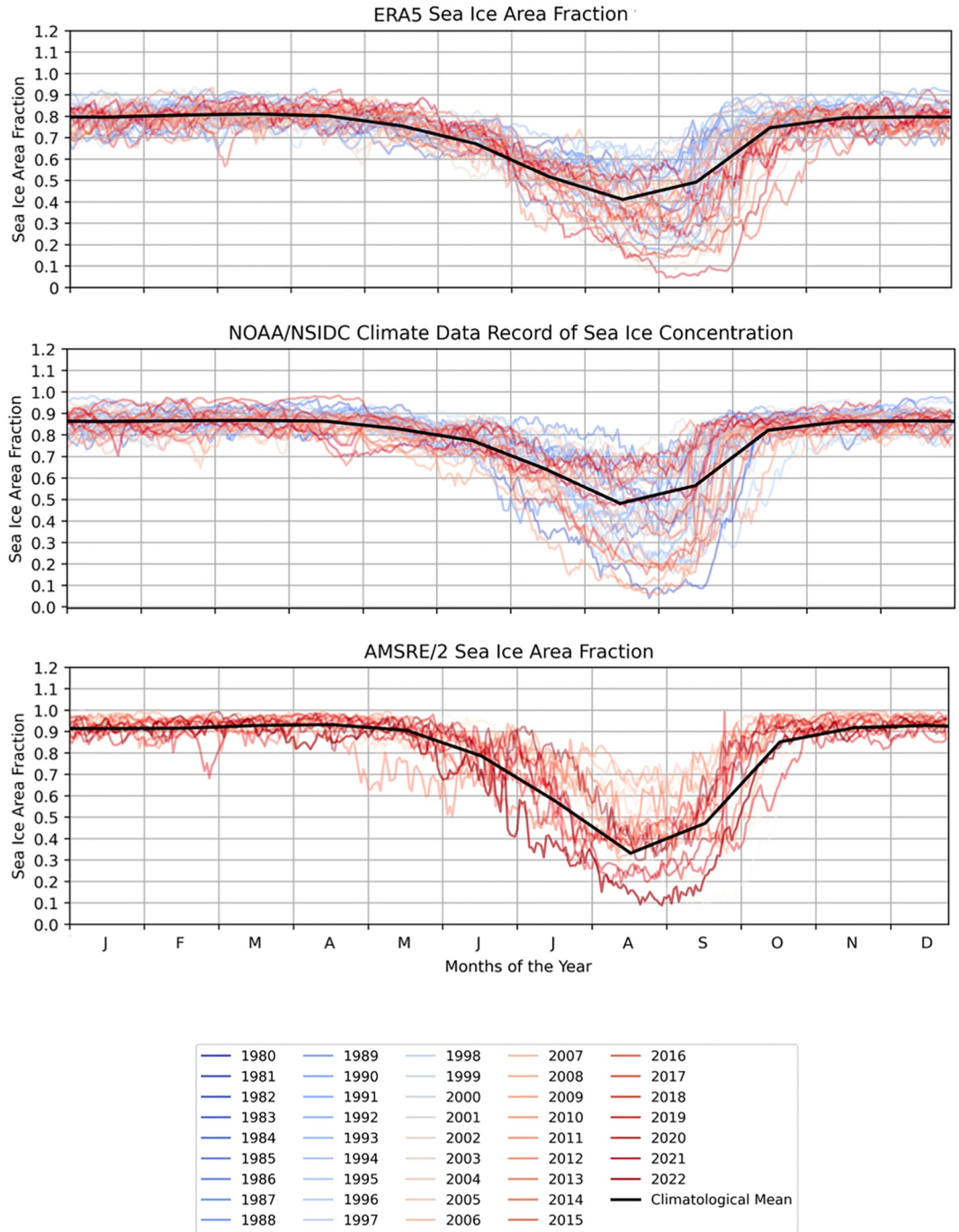

Figure A1. Daily sea-ice area fraction for each year for the Northeast Water Polynya yellow box region (shown in Figure 2) for ERA5, National Snow and Ice Data Center (NSIDC) (Climate Data Record) and Advanced Scanning Microwave Radiometer (AMSR) products as labeled.

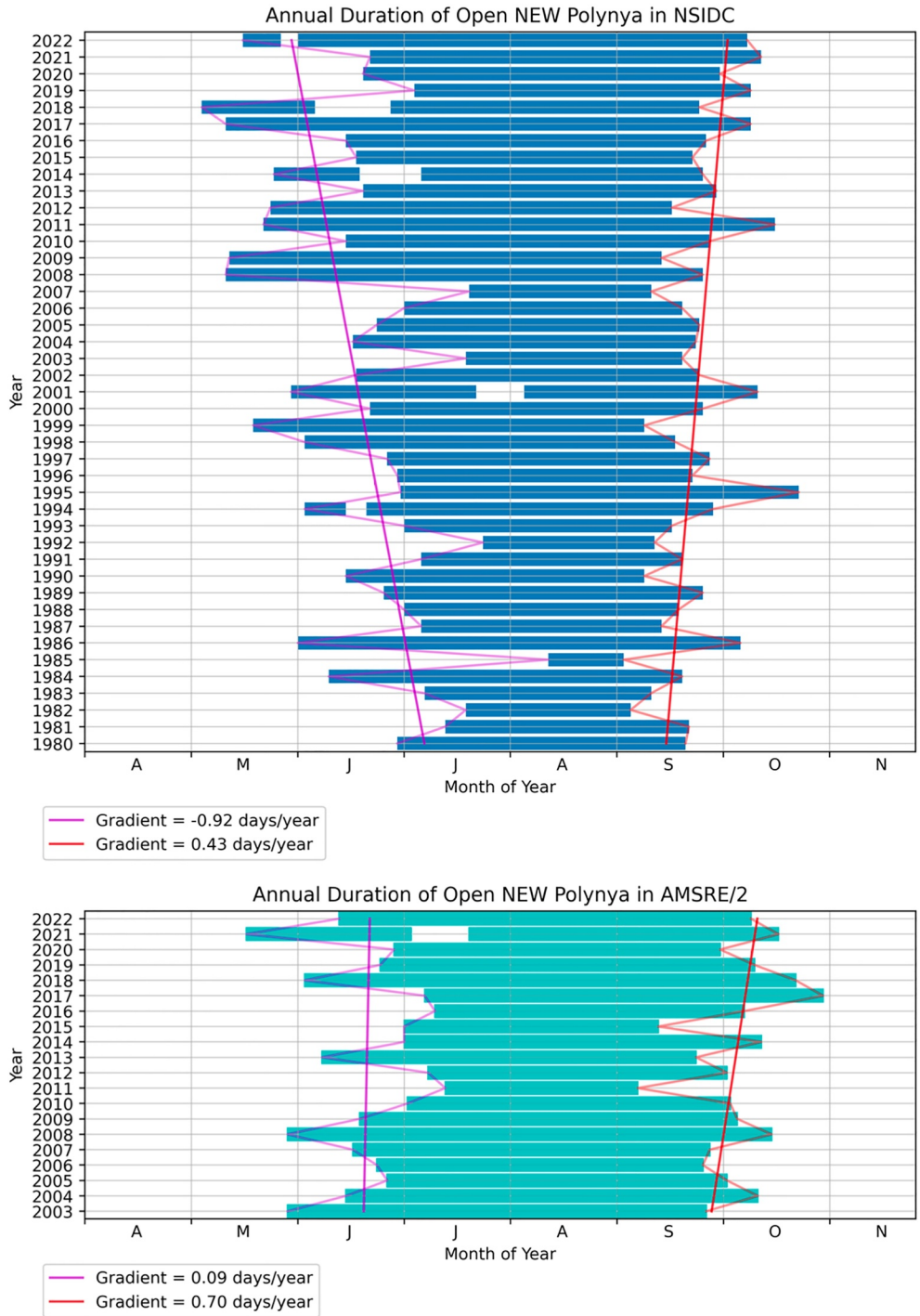

Figure A2. Annual timing of opening and closing of the Northeast Water Polynya based on sea-ice area fraction (for the yellow box in Figure 2) from National Snow and Ice Data Center (NSIDC) (Climate Data Record [CDR]) (upper panel) and AMSRE/2 (lower panel). Note that the Advanced Scanning Microwave Radiometer (AMSR) products are only available between 2003 and 2022, whereas the NSIDC (CDR) product is shown from 1980 to 2022. In both cases, a threshold value of 0.75 sea-ice area fraction for 10 or more consecutive days is used to represent the open polynya. The long-term trends in the opening and closing of the polynya are shown in magenta and red, respectively. For AMSR, the closing trend is statistically significant, where as for NSIDC the opening trend is statistically significant.

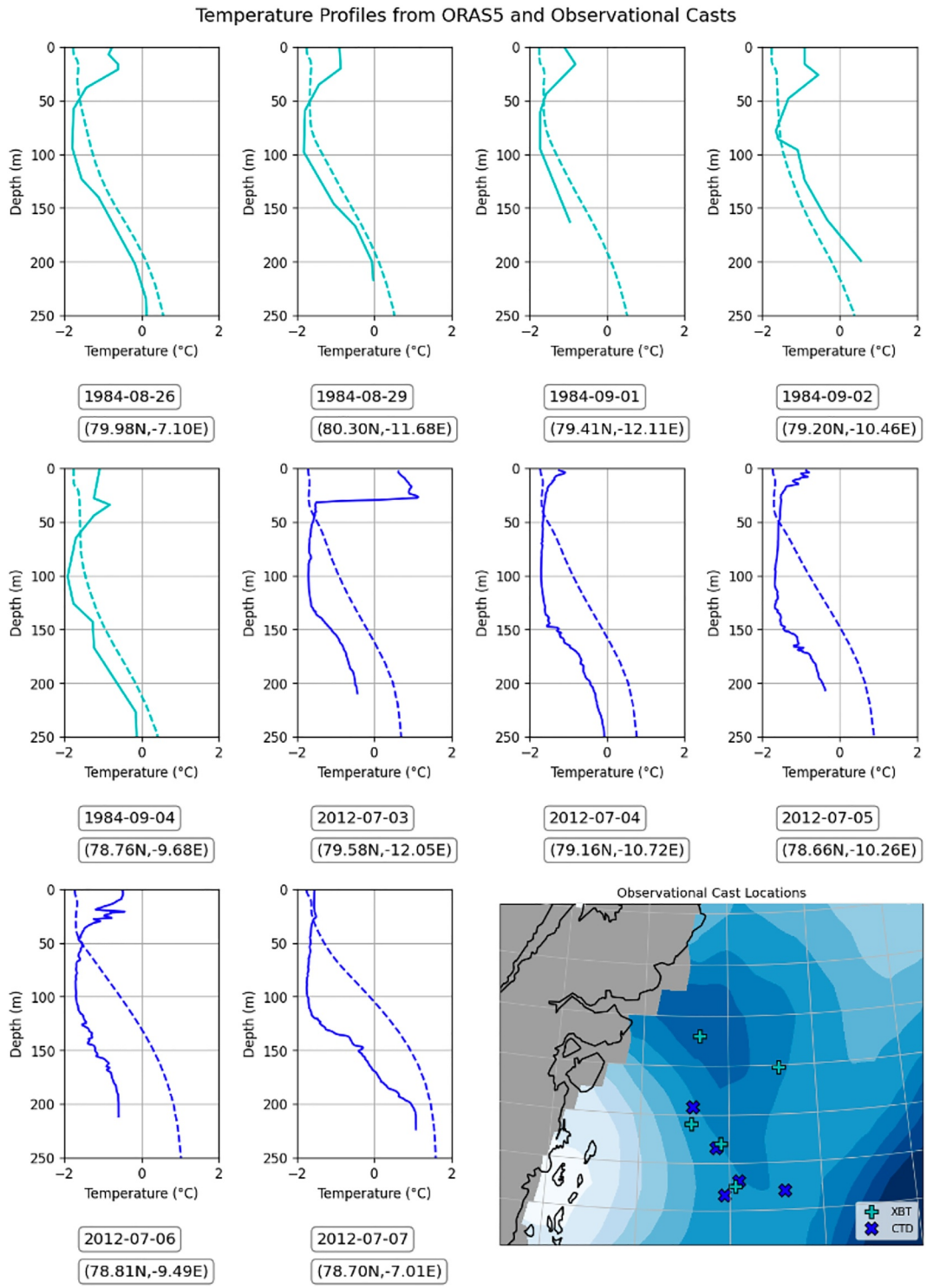

Figure A3. Temperature profiles from observational casts in the vicinity of the Northeast Water Polynya (solid lines) and the nearest equivalent in ORAS5 (dashed lines). The locations of the observational casts are shown on the inset map with the mean sea-ice area fraction from ERA5, averaged over the dates shown for the casts. The expendable bathythermograph and conductivity, temperature and depth casts are represented by the cyan and dark blue colors respectively.

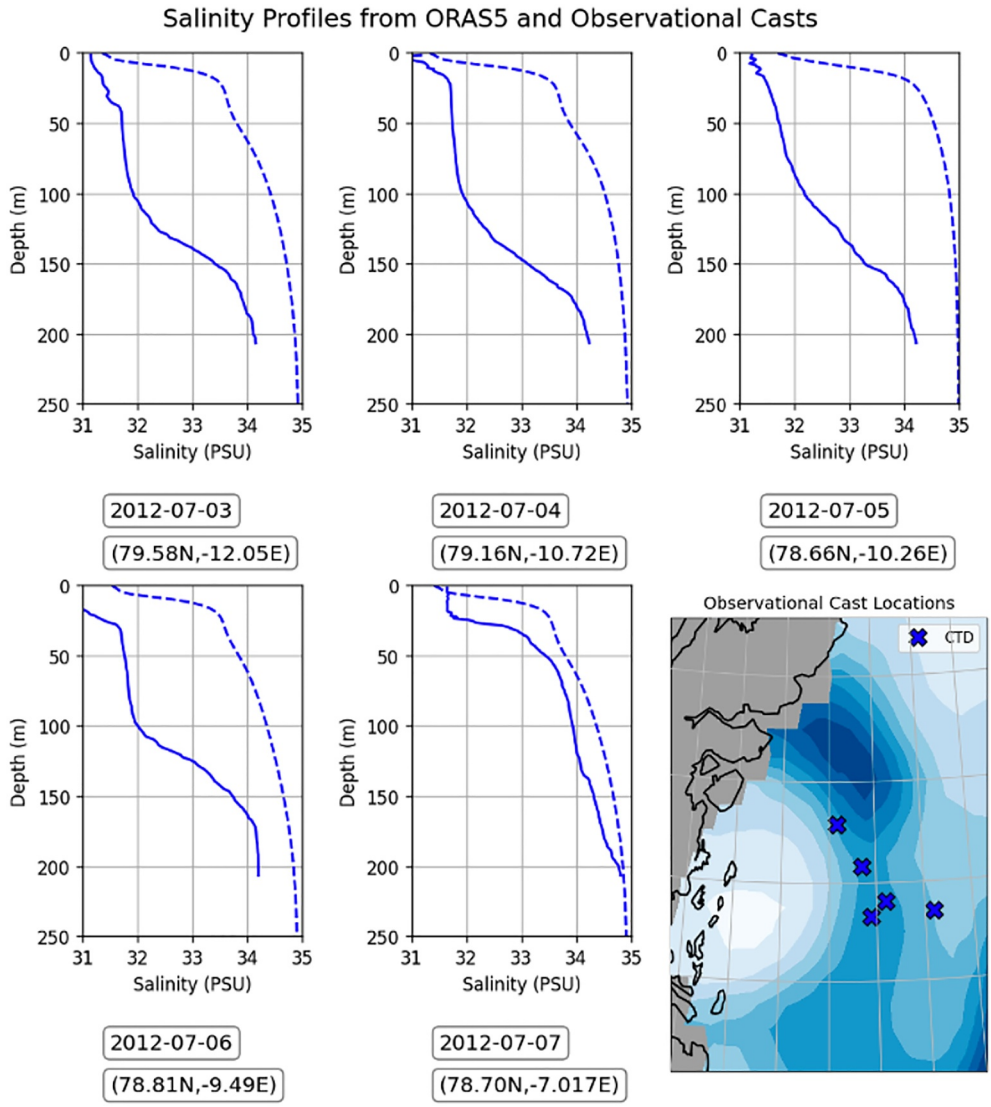

Figure A4. Salinity profiles from observational casts in the vicinity of the Northeast Water Polynya (solid lines) and the nearest equivalent in ORAS5 (dashed lines). The locations of the observational casts are shown on the inset map with the mean sea-ice area fraction from ERA5, averaged over the dates shown for the casts. The expendable bathythermograph and conductivity, temperature and depth casts are represented by the cyan and dark blue colors respectively.

Data Availability Statement

All ERA5 and ORAS5 data are available from the Copernicus Climate Data Store (https://cds.climate.copernicus.eu). AMSR-E and AMSR2 sea-ice data are available from the University of Bremen Remote Sensing webpage (https://seaice.uni-bremen.de/data-archive/) and the NOAA/NSIDC CDR of Passive Microwave Sea Ice Concentration (Version 4) is available online from NSIDC (https://nsidc.org/data/g02202/versions/4/). The observational ocean casts can be found on the World Ocean Database (https://www.ncei.noaa.gov/products/world-ocean-database). The bathymetry and topographic elevation data are available from GEBCO (https://www.gebco.net/data_and_products/gridded_bathymetry_data/) and USGS (https://www.usgs.gov/centers/eros#/Find_Data/Products_and_Data_Available/gtopo30_info) respectively. We used the GEBCO_2023 GRID (sub-ice topo/bathy) netCDF data set. MODIS satellite images can be found on the NASA Worldview webpage (https://worldview.earthdata.nasa.gov).

Acknowledgments
M.G.B. acknowledges support from the UK's Natural Environment Research Council (NERC) and the ARIES Doctoral Training Partnership (Grant NE/S007334/1). I.A.R. acknowledges partial support from Iceland Greenland Seas Project (Grant NE/N009754/1) and the Arctic Summertime Cyclones Project (Grant NE/T00682X/1). The research presented in this paper was carried out on the High-Performance Computing Cluster supported by the Research and Specialist Computing Support service at the University of East Anglia, UK. We would also like to thank three anonymous reviewers for their helpful feedback which has improved the final paper.

References

Asbjørnsen, H., Årthun, M., Skagseth, Ø., & Eldevik, T. (2020). Mechanisms underlying recent Arctic Atlantification. *Geophysical Research Letters*, *47*(15), e2020GL088036. https://doi.org/10.1029/2020gl088036

Barber, D., & Massom, R. (2007). The role of sea ice in Arctic and Antarctic polynyas. *Elsevier Oceanography Series*, *74*, 1–54. https://doi.org/10.1016/S0422-9894(06)74001-6

Böhm, E., Hopkins, T., & Minnett, P. (1997). Passive microwave observations of the Northeast Water Polynya interannual variability: 1978–1994. *Journal of Marine Systems*, *10*(1–4), 87–98. https://doi.org/10.1016/s0924-7963(96)00080-2

Budéus, G., & Schneider, W. (1995). On the hydrography of the Northeast Water Polynya. *Journal of Geophysical Research*, *100*(C3), 4287–4299. https://doi.org/10.1029/94jc02024

Cavalieri, D. J., Gloersen, P., & Campbell, W. J. (1984). Determination of sea ice parameters with the NIMBUS 7 SMMR. *Journal of Geophysical Research*, *89*(D4), 5355–5369. https://doi.org/10.1029/jd089id04p05355

Comiso, J. C. (1986). Characteristics of Arctic winter sea ice from satellite multispectral microwave observations. *Journal of Geophysical Research*, *91*(C1), 975–994. https://doi.org/10.1029/jc091ic01p00975

Dare, R., & Atkinson, B. (2000). Atmospheric response to spatial variations in concentration and size of polynyas in the Southern Ocean sea-ice zone. *Boundary-Layer Meteorology*, *94*(1), 65–88. https://doi.org/10.1023/a:1002442212593

Deming, J. (1993). Northeast Water Polynya: Polar sea cruise results. *Eos, Transactions American Geophysical Union*, *74*(16), 185–196. https://doi.org/10.1029/93eo00264

Ding, Y., Cheng, X., Li, X., Shokr, M., Yuan, J., Yang, Q., & Hui, F. (2020). Specific relationship between the surface air temperature and the area of the Terra Nova Bay Polynya, Antarctica. *Advances in Atmospheric Sciences*, *37*(5), 532–544. https://doi.org/10.1007/s00376-020-9146-2

Donlon, C. J., Martin, M., Stark, J., Roberts-Jones, J., Fiedler, E., & Wimmer, W. (2012). The Operational Sea surface Temperature and sea Ice Analysis (OSTIA) system. *Remote Sensing of Environment*, *116*, 140–158. https://doi.org/10.1016/j.rse.2010.10.017

Döscher, R., Vihma, T., & Maksimovich, E. (2014). Recent advances in understanding the Arctic climate system state and change from a sea ice perspective: A review. *Atmospheric Chemistry and Physics*, *14*(24), 13571–13600. https://doi.org/10.5194/acp-14-13571-2014

Eastwood, S., Lavergne, T., & Tonboe, R. (2014). Algorithm theoretical basis document for the OSI SAF global reprocessed sea ice concentration product In. *EUMETSAT Network Satellite Application Facilities* (Vol. 28).

Good, S., Fiedler, E., Mao, C., Martin, M. J., Maycock, A., Reid, R., et al. (2020). The current configuration of the OSTIA system for operational production of foundation sea surface temperature and ice concentration analyses. *Remote Sensing*, *12*(4), 720. https://doi.org/10.3390/rs12040720

Harden, B., Renfrew, I., & Petersen, G. (2011). A climatology of wintertime barrier winds off Southeast Greenland. *Journal of Climate*, *24*(17), 4701–4717. https://doi.org/10.1175/2011jcli4113.1

Hersbach, H., Bell, B., Berrisford, P., Hirahara, S., Horányi, A., Muñoz-Sabater, J., et al. (2020). The ERA5 global reanalysis. *Quarterly Journal of the Royal Meteorological Society*, *146*(730), 1999–2049. https://doi.org/10.1002/qj.3803

Hirano, D., Fukamachi, Y., Watanabe, E., Iwamoto, K., Mahoney, A. R., Eicken, H., et al. (2014). A wind-driven, hybrid latent and sensible heat coastal polynya at Barrow, Alaska. In *AGU fall meeting abstracts* (Vol. 2014, p. C11B–0371).

Holliday, N. P., Meyer, A., Bacon, S., Alderson, S. G., & de Cuevas, B. (2007). Retroflection of part of the East Greenland current at Cape Farewell. *Geophysical Research Letters*, *34*(7), L07609. https://doi.org/10.1029/2006gl029085

Iwamoto, K., Ohshima, K. I., & Tamura, T. (2014). Improved mapping of sea ice production in the Arctic Ocean using AMSR-E thin ice thickness algorithm. *Journal of Geophysical Research: Oceans*, *119*(6), 3574–3594. https://doi.org/10.1002/2013jc009749

Jeansson, E., Jutterström, S., Rudels, B., Anderson, L. G., Olsson, K. A., Jones, E. P., et al. (2008). Sources to the East Greenland current and its contribution to the Denmark Strait overflow. *Progress in Oceanography*, *78*(1), 12–28. https://doi.org/10.1016/j.pocean.2007.08.031

Karpouzoglou, T., de Steur, L., & Dodd, P. (2023). Freshwater transport over the Northeast Greenland shelf in Fram Strait. *Geophysical Research Letters*, *50*(2), e2022GL101775. https://doi.org/10.1029/2022gl101775

Klenke, M., & Schenke, H. W. (2002). A new bathymetric model for the central Fram Strait. *Marine Geophysical Researches*, *23*(4), 367–378. https://doi.org/10.1023/a:1025764206736

Koch, L. (1935). A day in North Greenland. *Geografiska Annaler*, *17*, 609–620. https://doi.org/10.2307/519888

Kottmeier, C., & Engelbart, D. (1992). Generation and atmospheric heat exchange of coastal polynyas in the Weddell Sea. *Boundary-Layer Meteorology*, *60*(3), 207–234. https://doi.org/10.1007/bf00119376

Ludwig, V., Spreen, G., & Pedersen, L. T. (2020). Evaluation of a new merged sea-ice concentration dataset at 1 km resolution from thermal infrared and passive microwave satellite data in the Arctic. *Remote Sensing*, *12*(19), 3183. https://doi.org/10.3390/rs12193183

Martin, S., & Cavalieri, D. J. (1989). Contributions of the Siberian shelf polynyas to the Arctic Ocean intermediate and deep water. *Journal of Geophysical Research*, *94*(C9), 12725–12738. https://doi.org/10.1029/jc094ic09p12725

Mattingly, K. S., Turton, J. V., Wille, J. D., Noël, B., Fettweis, X., Rennermalm, Å. K., & Mote, T. L. (2023). Increasing extreme melt in Northeast Greenland linked to föhn winds and atmospheric rivers. *Nature Communications*, *14*(1), 1743. https://doi.org/10.1038/s41467-023-37434-8

Maykut, G. A. (1982). Large-scale heat exchange and ice production in the central Arctic. *Journal of Geophysical Research*, *87*(C10), 7971–7984. https://doi.org/10.1029/jc087ic10p07971

Meier, W. N., Hovelsrud, G. K., van Oort, B. E., Key, J. R., Kovacs, K. M., Michel, C., et al. (2014). Arctic sea ice in transformation: A review of recent observed changes and impacts on biology and human activity. *Reviews of Geophysics*, *52*(3), 185–217. https://doi.org/10.1002/2013rg000431

Monroe, E. E., Taylor, P. C., & Boisvert, L. N. (2021). Arctic cloud response to a perturbation in sea ice concentration: The north water polynya. *Journal of Geophysical Research: Atmospheres*, *126*(16), e2020JD034409. https://doi.org/10.1029/2020jd034409

Moore, G., & Renfrew, I. (2005). Tip jets and barrier winds: A QuikSCAT climatology of high wind speed events around Greenland. *Journal of Climate*, *18*(18), 3713–3725. https://doi.org/10.1175/jcli3455.1

Moore, G., Våge, K., Renfrew, I., & Pickart, R. (2022). Sea-ice retreat suggests re-organization of water mass transformation in the Nordic and Barents Seas. *Nature Communications*, *13*(1), 67. https://doi.org/10.1038/s41467-021-27641-6

Morales Maqueda, M., Willmott, A., & Biggs, N. (2004). Polynya dynamics: A review of observations and modeling. *Reviews of Geophysics*, *42*(1), RG1004. https://doi.org/10.1029/2002rg000116

Ohshima, K. I., Nihashi, S., & Iwamoto, K. (2016). Global view of sea-ice production in polynyas and its linkage to dense/bottom water formation. *Geoscience Letters*, *3*(1), 1–14. https://doi.org/10.1186/s40562-016-0045-4

Polyakov, I. V., Pnyushkov, A. V., Alkire, M. B., Ashik, I. M., Baumann, T. M., Carmack, E. C., et al. (2017). Greater role for Atlantic inflows on sea-ice loss in the Eurasian basin of the Arctic Ocean. *Science*, *356*(6335), 285–291. https://doi.org/10.1126/science.aai8204

Renfrew, I. A., Barrell, C., Elvidge, A., Brooke, J., Duscha, C., King, J., et al. (2021). An evaluation of surface meteorology and fluxes over the Iceland and Greenland Seas in ERA5 reanalysis: The impact of sea ice distribution. *Quarterly Journal of the Royal Meteorological Society*, *147*(734), 691–712. https://doi.org/10.1002/qj.3941

Rudels, B., & Friedrich, H. J. (2000). The transformations of Atlantic water in the Arctic Ocean and their significance for the freshwater budget. In *The freshwater budget of the Arctic Ocean* (pp. 503–532).

Schauer, U., Fahrbach, E., Osterhus, S., & Rohardt, G. (2004). Arctic warming through the Fram Strait: Oceanic heat transport from 3 years of measurements. *Journal of Geophysical Research*, *109*(C6), C06026. https://doi.org/10.1029/2003jc001823

Sejr, M. K., Stedmon, C. A., Bendtsen, J., Abermann, J., Juul-Pedersen, T., Mortensen, J., & Rysgaard, S. (2017). Evidence of local and regional freshening of Northeast Greenland coastal waters. *Scientific Reports*, *7*(1), 1–6. https://doi.org/10.1038/s41598-017-10610-9

Smith, W., & Barber, D. (2007). Polynyas and climate change: A view to the future. *Elsevier Oceanography Series*, *74*, 411–419. https://doi.org/10.1016/S0422-9894(06)7401

Speer, L., Nelson, R., Casier, R., Gavrilo, M., von Quillfeldt, C. H., Cleary, J., et al. (2017). Natural marine world heritage in the Arctic Ocean: Report of an expert workshop and review process.

Spreen, G., Kaleschke, L., & Heygster, G. (2008). Sea ice remote sensing using AMSR-E 89-GHz channels. *Journal of Geophysical Research*, *113*(C2), C02S03. https://doi.org/10.1029/2005jc003384

Sutherland, D. A., & Pickart, R. S. (2008). The East Greenland coastal current: Structure, variability, and forcing. *Progress in Oceanography*, *78*(1), 58–77. https://doi.org/10.1016/j.pocean.2007.09.006

Tamura, T., & Ohshima, K. I. (2011). Mapping of sea ice production in the Arctic coastal polynyas. *Journal of Geophysical Research*, *116*(C7), C07030. https://doi.org/10.1029/2010jc006586

Tesi, T., Muschitiello, F., Mollenhauer, G., Miserocchi, S., Langone, L., Ceccarelli, C., et al. (2021). Rapid Atlantification along the Fram Strait at the beginning of the 20th century. *Science Advances*, *7*(48), eabj2946. https://doi.org/10.1126/sciadv.abj2946

Titchner, H. A., & Rayner, N. A. (2014). The Met Office Hadley centre sea ice and sea surface temperature data set, version 2: 1. Sea ice concentrations. *Journal of Geophysical Research: Atmospheres*, *119*(6), 2864–2889. https://doi.org/10.1002/2013jd020316

Van Angelen, J., Van den Broeke, M., & Kwok, R. (2011). The Greenland sea jet: A mechanism for wind-driven sea ice export through Fram Strait. *Geophysical Research Letters*, *38*(12), L12805. https://doi.org/10.1029/2011gl047837

Weijer, W., Haine, T. W., Siddiqui, A. H., Cheng, W., Veneziani, M., & Kurtakoti, P. (2022). Interactions between the Arctic mediterranean and the Atlantic meridional overturning circulation: A review. *Oceanography*, *35*(LA-UR-22-27688), 118–127. https://doi.org/10.5670/oceanog.2022.130

Yager, P. L., Wallace, D. W., Johnson, K. M., Smith, W. O., Minnett, P. J., & Deming, J. W. (1995). The Northeast Water Polynya as an atmospheric CO_2 sink: A seasonal rectification hypothesis. *Journal of Geophysical Research*, *100*(C3), 4389–4398. https://doi.org/10.1029/94jc01962

Zuo, H., Balmaseda, M. A., Tietsche, S., Mogensen, K., & Mayer, M. (2019). The ECMWF operational ensemble reanalysis–analysis system for ocean and sea ice: A description of the system and assessment. *Ocean Science*, *15*(3), 779–808. https://doi.org/10.5194/os-15-779-2019